

7—

Accessible Internal Volume Determination in Cotton

Noelie R. Bertoniere

Southern Regional Research Center, Agricultural Research Service, United States Department of Agriculture, New Orleans, Louisiana

I—

Introduction

Techniques based on the principles of gel permeation chromatography have found wide application since the initial report by Porath and Flodin [1] on the use of cross-linked dextran gel media of graded permeability. Such gels swell in water that penetrates pores differing in size. These pores are selectively more permeable to solutes of decreasing molecular size. Gels with a low level of cross-linking are used to separate macromolecules such as proteins, while those having a high degree of cross-linking are used to separate smaller molecules such as sugars and oligosaccharides.

In early investigations Aggebrandt and Samuelson [2], in a study aimed at determining nonsolvent water in cut and beaten cotton fibers, used six polyethylene glycols (MW = 60–20,000) as solutes with a centrifuge technique. They noted that the value calculated for nonsolvent water (δ) increased as the molecular weight of the glycol increased. They rationalized this based on the presence of pores of various sizes in the cotton fibers and postulated that determination with polyethylene glycols of varying molecular weights could be used to elucidate the pore size distribution in cellulose fibers.

Later Stone and Scallan [3] conducted static measurements based on the principle of solute exclusion to study the structures of the cell walls of wood pulps and celluloses. Their criteria for suitable solutes were that they must (1) not be sorbed onto the cellulose, (2) be available in a wide range of molecular weights, (3) be available as narrow molecular weight fractions, (4) be uncharged, and (5) be of known size and shape, preferably spherical. Based on these criteria they selected the low-molecular-weight sugars (glucose, maltose, raffinose, and stachyose) and a series of 11 dextrans (MW = 2600–24,000) to characterize the distributions of

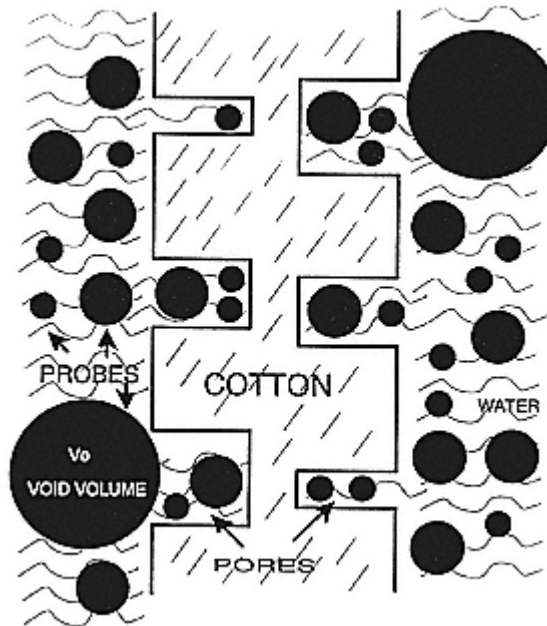


Figure 1
Simplified illustration of gel permeation mechanism.

pore sizes in wood pulps and celluloses. Based on evidence that predominantly linear dextrans behave as hydrodynamic spheres in solution, their molecular diameters, calculated from diffusion coefficients according to the Einstein-Stokes formula, were used. Calculations were based on changes in the concentration of the solute in the solution containing a known weight of the cellulose.

The basic principle upon which these, and the column chromatography method developed at the Southern Regional Research Center, are based is illustrated in an oversimplified manner in Figure 1. A very large molecule that cannot penetrate any of the pores in the cotton emerges from the cotton column first as it has a shorter path to traverse. In contrast, small molecules that can penetrate some of the accessible pores take a more circuitous route and thus emerge later. It is important to note that any of these methods can only assess the distribution of sizes in accessible pores. A pore that has no opening may exist but will not be detected by techniques based on gel filtration.

II—

Development of Reverse Gel Permeation Column Chromatography Method

The column chromatography technique developed to assess pore size distribution in cotton cellulose is the reverse of most gel permeation chromatography methods.

Here the sample is the column packing and the materials of known size are the solutes. It was developed, and evolved slowly, over a period of years, at the Southern Regional Research Center.

A—

Ball-Milled Cotton

Cotton cellulose is a highly crystalline material. Originally it was thought that a separation of solutes of different sizes could only be effected if the accessible, or amorphous, regions were increased by decrystallization. This was achieved by use of a vibratory ball mill by Martin and Rowland [4], who first reported that this decrystallized cotton cellulose had gel permeation properties comparable to highly cross-linked dextran. The sugars used as probes were erythrose, fructose, maltose monohydrate, raffinose pentahydrate, and stachyose tetrahydrate. Solute emerging from their column were detected with a sensitive automatic polarimeter that distinguished between dextrorotatory and levorotary sugars. In a following report these authors [5] compared decrystallized cotton prepared from desized, scoured and bleached cotton printcloth with the decrystallized cotton after it had been cross-linked with formaldehyde in the swollen state. They found that although cross-linking reduced permeability to large molecules, the cross-linked material was more permeable than the untreated cellulose to compounds having molecular weights below 1000.

Work with ball-milled cotton continued [6] with a comparison of unmodified cotton, methylated cotton, cotton cross-linked with formaldehyde in the swollen and collapsed states, and microcrystalline wood cellulose. A differential refractometer replaced the polarimeter, and a siphon with a photoelectrically actuated mechanism for marking the recorder chart was added to the system. Fractions were collected and weighed. Relative elution volume was defined as the differences between the elution volume of the sugar and the void volume divided by the weight of cellulose in the column. Plots were made of the relative elution volumes against the molecular weights of characteristic crystalline hydrates of the sugars. The effective internal solvent volume (intercept where molecular weight equals zero) and the apparent limit of permeability (the molecular weight of a solute just large enough to be completely excluded from the gel) were extrapolated from this linear relationship. It was concluded that cellulose cross-linked in the swollen state exhibited increased permeability, whereas cross-linking under conditions that minimize swelling increased the internal volume while causing a decrease in the limit of permeability. Monofunctional substitution, with the methyl group here, increased the internal volume to the same extent as cross-linking in an unswollen state while increasing the limit of permeability. The microcrystalline wood cellulose was found to have as large an internal volume as decrystallized cotton cellulose, but a much higher limit of permeability. The large internal volume was surprising as the microcrystalline wood cellulose was a commercially modified material produced by controlled acid hydrolysis, which is assumed to have re-

moved amorphous cellulose. Its "microcrystalline" nature was confirmed by x-ray scattering. The high permeability limit, almost twice as large as that calculated for decrystallized cotton cellulose, indicated that considerably less of the total internal volume is distributed in intermolecular spaces that are accessible only to molecules of smaller sizes.

This study was extended [7] to include the effects on the structure of decrystallized cotton produced by introduction of formaldehyde cross-linked under various reaction conditions. These included reaction in aqueous solution, in the vapor phase, in acetic acid, and in a bake-cure process. The experimental techniques and data handling for pore size distribution assessment remained the same. It was shown that accessibility was increased by reaction in aqueous solution, that reaction catalyzed by hydrochloric acid in the acetic acid medium formed products having larger internal volumes, but somewhat lower limits of permeability, and that both the internal volume and the permeability limit were decreased by the bake-cure process. A related study [8] reported changes in the permeation characteristics of cotton as a function of the levels of formaldehyde crosslinking achieved under bake-cure conditions and in the acetic—hydrochloric acid medium. Marked differences were found in the pore structures of the cotton cross-linked to progressively higher levels with both processes.

B—

Sephadex as a Model for Cellulose

One of the major experimental problems with columns made from cotton cellulose decrystallized by ball milling was column instability. The flow rate gradually decreased to the point where usable data could not be obtained. Because commercial, highly cross-linked dextrans behave like cellulose in the way they discriminate among low-molecular-weight sugars, two basic studies were conducted with Sephadex G-15 as a model for cellulose. In the first, Bertoniere et al. [9] studied the elution of sugars and sugar derivatives relative to glucose (R_g) to determine the effect of stereochemical and structural differences between molecules of approximately the same size. The following observations were made: (1) the gel could not distinguish between enantiomeric saccharides, (2) a decrease in R_g values was observed on going from a methylene to a hydroxyl to a methoxyl group in monosaccharides, (3) methylation or reduction of a particular hydroxyl group affects the R_g values selectively, (4) the substituted (methyl or glucosyl) α anomer is retained on the column longer than the corresponding β anomer, and (5) sugars having either one or no axially attached hydroxyl groups are eluted in the order: axially attached hydroxyl groups at C-4, at no carbon atom, at C-2, and at C-3. Thus the linear inverse relationship between the elution volumes and molecular weights of the characteristic hydrates of glucose, maltose, raffinose, and stachyose is fortuitous. It is nonetheless very useful as it permits the comparison of changes in the pore size distribution in cotton samples.

The original criterion of Stone and Scallan [3] was that solutes not be sorbed onto the cellulose if they are to be used as "feeler gauges." We therefore explored and reported [10] the interaction of several classes of solutes with the dextran gel Sephadex G-15, which was used as a model for cellulose. Solute classes included a variety of sugars, methylated sugars, polyethylene glycols, polyethyleneimines, and derivatives of 2-imidazolidinone (ethyleneurea). The last class of compounds is of high practical interest because they form the basis for conventional cross-linking agents for cotton to impart easy care properties. It was found that low-molecular-weight polyethylene glycols were eluted in much smaller volumes than sugars having comparable molecular weights. The 15 2-imidazolidinone derivatives showed no simple relationship of elution volumes to molecular weights, but sorption via hydrogens on the ring nitrogen atoms appeared to be a factor. This had strong implications with respect to the interactions between these compounds and cotton cellulose in chemical finishing. Polyethyleneimines were sorbed so strongly on the column that they could not be eluted with water.

A third study [11] elucidated the interactions of several water-soluble solutes with both Sephadex G-15 and cotton. Water-soluble solutes included simple sugars, their completely methylated analogues, glucuronic and galacturonic acids, oligomers of ethylene glycols and their dimethyl ethers (glymes), and a series of 2-imidazolidinones. The following conclusions were drawn. Total pore water becomes available as solvent water to polysaccharides and polyethylene glycols as the molecular sizes of these solutes decrease toward and approach that of water; all water in a pore that is accessible to these polysaccharides or polyethylene glycols is available to the solutes as solvent water. Water-soluble solutes characterized by more limited hydrogen-bonding capabilities than saccharides and polyethylene glycols find only a fraction of the total water in accessible pores available as solvent water; the nonsolvent water is that which remains structured and bound on cellulosic or polysaccharidic surfaces. Water-soluble solutes that are characterized by hydrogen donor and acceptor strengths that are higher than those of saccharides and polyethylene glycols find all water in an accessible pore available as solvent water, and these solutes interact with the cellulosic or polysaccharidic surfaces in proportion to the strength of hydrogen bonding and the number of hydrogen-bonding sites in the solute. Permeation of water-soluble solutes into pores of cellulose or insoluble polysaccharides is influenced by electrostatic charge in the solutes, with cationic and anionic charges contributing to positive and negative sorption, respectively.

C—

Chopped Cotton Fibers

Interactions between solutes in aqueous media and cellulose are the essence of chemical modification of cotton. Practical modifications of this fiber are usually conducted on the fabric where the desized, scoured and bleached fibers are intact.

Decrystallization by ball milling alters the molecular structure and reduces the degree of polymerization of cotton cellulose to approximately 500. Data on the pore size distribution in the cotton fiber would ideally be obtained on the whole, or at least minimally disturbed, fiber. In order to approach this ideal Blouin et al. [12] chopped the cotton fabric in a Wiley mill to pass successively through 20-, 40-, 60-, and 80-mesh screens. This shortened the fibers without causing significant decrystallization. Larger columns, holding three times as much cellulose, were used. They reported that crystalline cotton had an apparent internal volume approximately 53% of that of decrystallized cellulose. The molecular weight limit of permeability was 2900, compared to approximately 1900 for the decrystallized material. The work was extended with an investigation into the effect of mercerization, conducted on fibers that had been chopped to pass through the 20-mesh screen; reduction in size was complete on the mercerized fibers. Mercerization was reported to increase the apparent internal solvent volume by approximately 60%, but to decrease the limit of permeability to a molecular weight of 2200.

Following up on this initial report, Blouin et al. [13] used the new technique for evaluating fibrous cotton to study changes in structure from cross-linking with formaldehyde. In this study the cross-linking treatments were applied to fabric that was subsequently reduced by Wiley milling to the particle size required for uniform packing of the columns. The object of the study was to determine the pore structure of cotton cellulose following cross-linking with formaldehyde in typically wet-cure and bake-cure reactions. The state of distension of the accessible regions of the fibers at the time of cross-linking differs under the two reactions conditions and was expected to be reflected in the gel permeation properties of the cross-linked cottons. Cross-linked compositions were examined at progressively higher levels of formaldehyde contents, which were obtained under various reaction conditions. Cotton was cross-linked in a water-swollen state by both the Forms W and W' processes, which differ primarily in the higher concentration of reagent and lower concentration of water present in the latter. The fabric was cross-linked in the collapsed state by a bake-cure reaction, Form C. These cross-linked samples were prepared in a single curing step with $MgCl_2 \cdot 6H_2O$ as the catalyst. The wet-cure processes Form W and W' produced only limited alterations of the cellulose pore structure at the maximum levels of cross-linking. In contrast, large changes in pore structure resulted from cross-linking the cotton in a collapsed state by the bake-cure Form C process. Here, the permeability limit was reduced from a molecular weight of 2430 for untreated cotton to approximately 1250 at the lowest level of cross-linking achieved. No further decrease of this parameter was produced by cross-linking to the maximum level.

D—

Whole Fiber Cotton

The chemical modification of cotton fabric involves treatment of cotton cellulose in a whole fiber form. Wiley milling as described earlier, while producing a fibrous

product, does introduce undesirable perturbations in this crystalline polymer. It was therefore desirable to develop a technique for preparing columns from whole-fiber cotton without chopping to pass an 80-mesh screen. The trial studies [14, 15] were conducted on sterile absorbent cotton, Soxhlet extracted sliver, roving, and yam, and desized, scoured and bleached cotton printcloth. Among the various trial preparations of columns were (1) settling of loose fibers into a column, (2) random or ordered packing of chunks, balls, and sliver, (3) ordered wrapping of sliver, roving, yarn, and fabric prior to or during insertion into the column, and (4) ordered packing of die-cut disks. It is essential that packing be even. Methods 1–3 did not produce usable columns. Method 4 was first applied to cotton fabric. The die cut disks were exactly the same diameter as the interior of the column. The column was prepared with the fabric running perpendicular to the length of the column. Channeling was a problem, probably because the fabric construction restricted fiber swelling. The most satisfactory technique involved die-cut disks of batting. These dry disks of parallel fibers were pressed together into the column with a dowel rod, taking care to maintain fiber orientation perpendicular to the column's length. After wetting, additional compression allowed the addition of more disks. Such columns give usable data, but peaks are broader than those observed with either Sephadex G-15 or chopped cotton. The advantage is that one is able to assess the pore size distribution in cotton that has had minimal mechanical perturbation.

The technique was first used to assess changes in cotton effected by caustic mercerization and liquid ammonia treatment. The starting batting was sterile absorbent cotton batting. Caustic mercerization was with 23% NaOH at room temperature. Liquid ammonia treatment involved evaporation of almost all of the ammonia before quenching with and rinsing in water. Columns were characterized with the series of sugars, ethylene glycols, and glymes. Results showed that accessible solvent water in the pores was lowest for the untreated cotton, highest for the caustic mercerized cotton, and intermediate for the liquid ammonia-treated cotton. There were general similarities but small quantitative differences for results from chopped and whole-fiber cottons, as would be expected. This procedure represented a substantial advance in this endeavor and a real improvement in column stability.

E—

Fabric

Two different techniques have been described by other investigators for evaluating the pore size distribution in cotton fabric. The work of Bredereck et al. [16] is summarized in a recent review. These investigators cut discs of fabric that matched the column diameter exactly. The discs were introduced under gentle pressure into an HPLS steel column of 250 mm length and 4 mm internal diameter. The weight of the filling was approximately 2 g and the intermediate fiber volume 1.1–1.5 ml. This parameter was determined via the elution of Dextran T-2000. A double-piston pump with high pulsation and constant flow delivered the eluents. A Rheodyne

7125 sample application valve and LCD 202 RI detector completed the setup. The solutes were applied as 0.02 ml of 1% aqueous solutions (0.5% for dextrans of molecular weight greater than 40,000). The eluent was double-distilled water. Test samples were applied individually, and elution volumes were determined via peak maxima. Under normal circumstances columns were stable for 6 months. This technique was used to elucidate the effects of several finishing treatments on cotton fabric. These included cold and hot caustic mercerization, liquid ammonia treatment with ammonia removal both by rinsing in cold water and by dry evaporation on hot cylinders, and dry cross-linking with 1,3-dimethylol-4,5-dihydroxyethyleneurea.

Ladisich et al. [17] have reported a different liquid chromatography technique for studying the pore volume distribution in fabrics. They described a method for using a whole piece of fabric rolled into a cylinder. The fabric was rolled tightly along the warp direction and then pulled into a standard 7 mm i.d. \times 300 mm LC column. The tightness of the packing was demonstrated via scanning electron microscopy. Experimentally the system includes a water reservoir, a pump adjusted to flow at a rate of 0.20 ml/min, a syringe loading sample injector (20 μ l), the column immersed in a circulating water bath, a differential refractometer, and a chart recorder. These authors use different notations than those employed by Bertoniere et al. A brief summary follows.

Bertoniere et al.	Ladisich et al.
V_0 Void volume; from Dextran T40	V_ϵ External void volume; from Dextran T40
v_e Elution volume	$V_{r,i}$ Elution volume
V_i Internal water available as solvent to a specific solute	V_i Void Volume; specific accessible internal void volume corresponding to probe of specific diameter

Results for cotton and ramie fabrics were reported in this initial publication. Nine polyethylene glycols (in a series) were used as molecular probes. The values of Nelson and Oliver [20] for their molecular diameters were used. The fabrics were evaluated at both 30 and 60°C. It was shown that cotton had 100–200% more void volume (V_i) than ramie. The total void volume (V_i) of both cotton and ramie was not sensitive to temperature changes in the range of 30–60°C. The results of Ladisich et al. are in agreement with published data [15]. Subsequent studies using this liquid chromatography method on whole fabric by Ladisich et al. involved dyeability. They obtained direct dye absorption isotherms using a rolled cotton fabric stationary phase in a liquid chromatographic column [18]. A frontal analysis technique gave results similar to those obtained with standard equilibrium adsorption

measurements. In a later report [19] frontal analysis provided retention volumes of basic dyes on acrylic fabric, rolled and inserted into a liquid chromatographic column. The retention volumes indicated differences in adsorption and therefore in compatibilities of standard dye mixtures.

III— Current Methods Used at SRRC to Characterize Cotton

A— Equipment

The system is assembled from separately purchased commercial units as shown in Figure 2. Component parts include columns, a sample injector, a pump, a differential refractometer detector, a recorder, a fraction collector, tared test tubes, and a precision balance. The columns used must be precision bore with dimensions

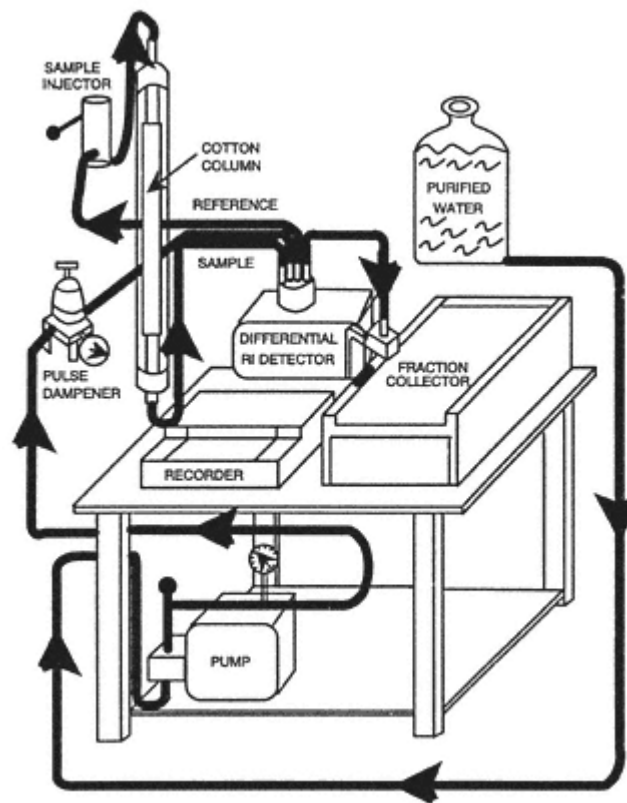


Figure 2
Diagram of assembled equipment used at SRRC.

2.54 (or 1.27) cm \times 45–50 cm between top and bottom bed supports. The sample injector must be capable of delivering 0.5 ml to the column without interruption of flow. The pump should provide a flow rate of ~ 26 ml/cm²/hr; pulse dampening is usually necessary with the positive-displacement minipumps we have used.

B—

Column Preparation

In order to prepare columns from whole cotton fibers a batting with parallelized fibers is prepared on a card. Disks are cut from the batt with a die having precisely the same diameter (2.54 or 1.27 cm) as the interior of the column. The column is packed with the die-cut disks in the dry state. These fiber disks are pressed together with a dowel rod, taking care to retain the configuration of fiber lengths running perpendicular to the length of the column. After the column is wetted down, the disks are further compacted with the dowel rod and additional fiber disks are added. It is essential that the maximum amount of cotton be used in the column and that both top and bottom bed supports make good contact with the cellulose. The column is placed in the system and water is pumped through it until all trapped air is removed. This can take several days.

In order to evaluate fabric we found it necessary to grind it in a Wiley mill as discussed earlier, as our attempts to pack our columns with fabric disks of the same diameter as the interior of the column failed because of channeling, particularly if the cotton was cross-linked. Therefore the fabric was successively passed through 20-, 40-, 60-, and 80-mesh screens in a Wiley mill. The ground fabric was placed in water and the slurry was degassed. The columns were prepared by settling the cotton slurries through an extension tube in the conventional manner. Normally the 2.54-cm-diameter columns were used, but we have also been successful with 1.27-cm-diameter columns, which require substantially less sample. Other investigators [16, 17] have reported success in preparing columns from intact fabric using other equipment as described earlier.

C—

Evaluation

The water-soluble solutes used routinely as molecular probes are assembled in Table 1. Plots of the internal water available as solvent to a specific solute (V_i) versus its molecular weight are linear in the case of the sugars but curvilinear for both the ethylene glycols and the glymes. Within a homologous series, molecular weight is a good measure of relative molecular size. A molecular size basis is preferable when making comparison with different series of solutes. The molecular diameters of the sugars have been reported by Stone and Scallan [3]. Estimates of the molecular diameters of the lower molecular weight ethylene glycols were based on extrapolations from measurements of Nelson and Oliver [20]. Measurements of molecular diameters were not available for the glymes but were approximated by assuming that molecular sizes of the hydrated molecules are the same

Table 1 Molecular Probes Used in Reverse Gel Permeation Chromatography

Molecular probe	Molecular weight	Molecular diameter (Å)
Dextran T-40 (void volume)	40,000	
Sugars		
Stachyose	666.58	14
Raffinose	504.44	12
Maltose	342.30	10
Glucose	180.16	8
Ethylene glycols, degree of polymerization		
6	282.33	15.6
5	238.28	14.1
4	194.22	12.7
3	150.17	10.8
2	106.12	8.4
1	62.07	5.5
Glymes, degree of polymerization		
1	222.28	13.8
2	178.22	12.1
3	134.17	9.9
4	90.12	7.4

as those of the parent glycols at the same molecular weight. Plots of V_i versus molecular diameter are linear for all three sets of molecular probes.

Dextran T-40, the sugars, and the ethylene glycols were applied individually as 2% solutions through a 0.5-ml sample loop. The flow rate was 26 ml/cm²/hr. The eluate was monitored continuously with an LDC differential refractometer from Milton Roy. Elution volumes were determined gravimetrically by collecting the eluate in tared test tubes and summing the weights of fractions and proportional parts of fractions between the injection and the peak of the recorded elution curve for each solute. Gel permeation chromatographic results are obtained in terms of:

V_e , elution volume for each specific substrate

V_0 , total void volume for the column

V_p , the total column volume

W, the weight (dry basis) of material in the column.

The total void volume V_0 is the elution volume of the high-molecular-weight solute Dextran T-40, molecular weight 40,000, which is totally excluded from the internal pore structure. Calculated results are expressed as accessible internal vol-

ume V_i (ml/g), specific gel volume V_g (ml/g), and internal water V_w (ml/g). These terms (per gram dry cellulose) were defined by the following equations [11]:

$$V_i = (V_e - V_0)/W$$

$$V_g = (V_t - V_0)/W$$

$$V_w = V_g - 0.629$$

The specific volume occupied by the solid cellulose in the water-wet fiber (required to calculate V_w) was taken as 0.629 ml/g, which corresponds to a density of 1.59 g/ml [21].

D—

Plots

V_i values are typically the averages of six replicates. Standard deviations are generally in the order of 0.001 to 0.01. Data (V_i vs. the molecular diameter of the test solute) are fit to linear regression models. The three sets of molecular probes give similar but not identical results, as shown in Figure 3. Results for pores accessible to small or moderate-sized molecules consistently fall in the order sugars > ethylene glycols > glymes. The sugars, relatively stiff and bulky molecules, are very similar to cellulose itself in hydrophilicity and hydrogen bonding power [15]. These solutes are thus competitive with cellulose for bound water within the pores of cotton and find all of the internal water available as solvent. The ethylene glycols, more flexible, slender molecules, contain both a hydroxyl group and an ether oxygen. While their greater flexibility would result in better penetrating power, they would compete less successfully for internal bound water and find a smaller

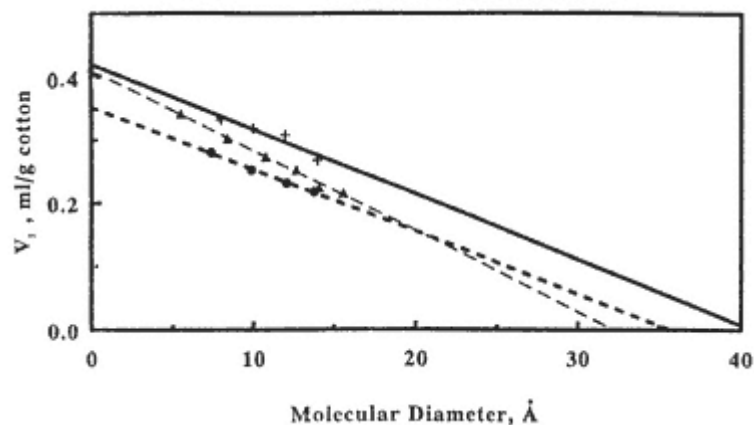


Figure 3
Differences in the internal volume of unmodified cotton available as solvent to the sugar (+), ethylene glycols (▲), and glymes (●).

fraction of it available as solvent. The glymes contain only ether structures, and the internal water available to small molecules is substantially lower than that of the parent ethylene glycols.

Useful predicted values for V_{2} , V_{10} , V_{16} , C_{21} , and V_{27} have been calculated as the mean of V_i when molecular diameter was 2 (water), 10 (typical cross-linking agent), 16 (polyethylene glycol, molecular weight 300), 21 (polyethylene glycol, molecular weight of 600), and 27 (polyethylene glycol, molecular weight of 1000), respectively. Predicted values for molecular diameter when $V_i = 0$ gives M_x , the permeability limit. This is the smallest molecule indicated to be excluded from the fiber interior.

IV—

Structures Elucidated

A—

Cotton Variety

Cotton fibers are seed hairs of plants belonging to the genus *Gossypium*. Each variety produces a characteristic type of fiber. *Gossypium barbadense* is a long staple type whereas *Gossypium hirsutum* is coarser. American upland cottons (*G. hirsutum*) account for most of the world fiber supply. Pima, a *G. barbadense* that is a complex cross of several cottons, contributes to the remainder. It is grown primarily in the southwestern United States. Different varieties of cotton are known to differ in many physical properties such as staple length, diameter, strength, elongation, toughness, and color. Potential differences in supramolecular structure have been less fully elucidated.

The reverse gel permeation chromatography technique was used to address differences in the pore structures of two varieties of cotton [22]. The varieties were DP-90 (a common upland variety) and NX-1 (a hybrid of upland and Pima cottons). Ginning was done on a small laboratory gin. Pore structure was assessed on the greige cottons in both the whole and ground states. The series of oligomeric sugars and ethylene glycols were used as molecular probes. Ground samples consistently had more accessible internal volume than the whole fibers across the entire range of pore sizes. This is attributed to damage effected by the grinding procedure. General differences between the two varieties were the same regardless of the physical state of the fiber in the column. The DP-90 had the more open structure across the whole range of pore sizes. This is illustrated in Figure 4 with data for the whole fibers. The chromatographic results were compatible with results from water of imbibition [23], which is related to internal volume in the water swollen state.

B—

Bast Fibers

Another study [24] extended the use of this technique to jute, a lignocellulosic bast fiber. The pore structures of jute and purified cotton cellulose were compared and

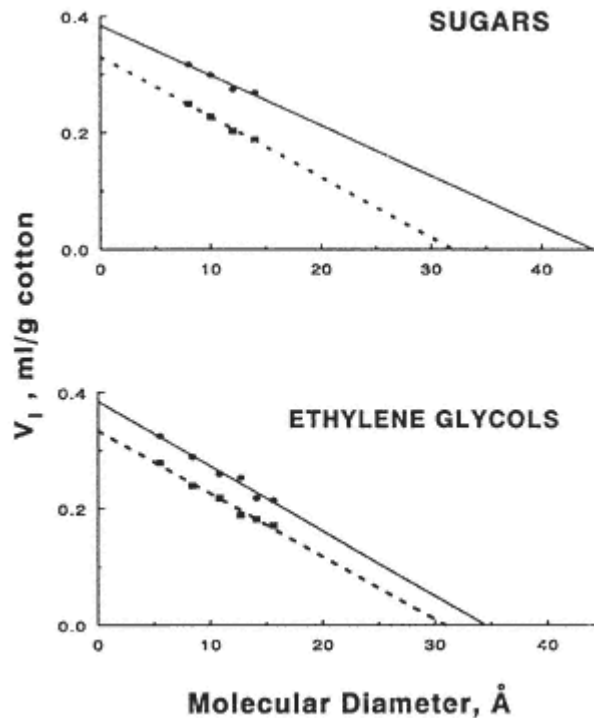


Figure 4
Differences in the pore size distribution
between the cotton varieties
NX-1 (■) and DP-90 (●).

the effect of scouring on jute was determined. Both native and scoured jute had greater pore volumes than purified cotton. Scouring effected an increase in the internal volume of the jute fiber over the measured range of pore sizes. Data on the fraction of the total internal water volume accessible to the water molecule itself indicated a similarity between cotton and scoured jute, but these and other data suggested a repelling interaction between the surfaces on the internal pores of native jute and the sugars used as test solutes. This repellent effect was attributed to the presence of lignin on these surfaces.

C—

Pretreatments

Prior to chemical modification with various agents cotton fabric is routinely desized, scoured, and bleached. Scouring imparts the required wettability by removing the natural waxes and the sizing agent applied to facilitate fabric construction. Bleaching renders the fabric white so that it can be dyed true to color. In many instances swelling pretreatments are utilized to improve dimensional sta-

bility, dyeability, luster, softness, and textile performance. Such pretreatments include caustic mercerization and liquid ammonia treatment. To study changes in pore size distribution caused by these pretreatments, columns prepared from whole cotton fibers in the form of batting were used [25, 26]. The treatments included standard scouring/bleaching, caustic mercerization, and a liquid ammonia treatment with removal by volatilization at elevated temperature. Results were compared to data on the pore structure of the fiber in the greige state. The water holding capacities of these fibers as measured by water of imbibition, specific internal water V_w , and V_2 (sugars) as assembled in Table 2. Scouring/bleaching decreased the water holding capacity of the greige cotton as measured by water of imbibition and the column parameter V_w but increased it as indicated by gel permeation measurements. The internal volume accessible to water was substantially increased by caustic mercerization but was only slightly affected by liquid ammonia treatment. The gel permeation data are given in Figure 5. The relative accessibility of the cotton fibers to molecules of the size of durable press finishing agents ($\sim 10 \text{ \AA}$) was slightly increased by scouring/bleaching, substantially increased by caustic mercerization, but moderately reduced by liquid ammonia treatment. Accessibility to molecules near the permeability limits of the fibers followed similar trends but differences were greater. Scouring/bleaching increased the permeability limit of the greige fibers, but subsequent mercerization or liquid ammonia treatment decreased it. There was a noteworthy difference in permeability limit and relative accessibility to large molecules. This is accounted for by a decrease in the rate of change in pore size on scouring/bleaching but substantial increases, to generally more than double, on subsequent caustic mercerization or liquid ammonia treatment of the scoured/bleached cotton.

Processing in liquid ammonia causes complex changes in the cotton fiber that are only partially understood. Liquid ammonia penetrates the cotton fiber, effect-

Table 2 Water-Holding Capacity of the Cotton Fibers as Indicated by Water of Imbibition and Gel Permeation Measurements (All Values in ml water/g Cotton)

Batting	Water of imbibition	V_w	$V_{2 \text{ sugars}}$	V_2 ethylene glycols
Greige control	0.337 ± 0.004	0.340 ± 0.004	0.316 ± 0.003	0.291 ± 0.002
Scoured/ bleached	0.334 ± 0.006	0.297 ± 0.006	0.319 ± 0.004	0.307 ± 0.004
Caustic mercerized	0.540 ± 0.008	0.557 ± 0.002	0.598 ± 0.008	0.356 ± 0.001
Ammonia treated	0.348 ± 0.012	0.357 ± 0.004	0.357 ± 0.005	0.300 ± 0.002

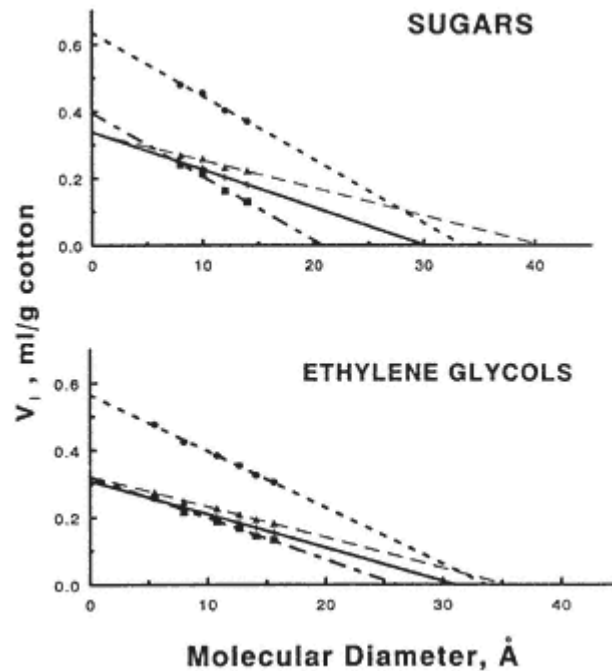


Figure 5
Changes effect in the pore size distribution
of greige cotton (+) effected by
scouring/bleaching (▲), caustic
mercerization (●), and liquid ammonia
treatment with dry removal (■).

ing intra- and inter fibrillar swelling, which disrupts the hydrogen bond structures and leads to the formation of a cellulose—ammonia complex. Destruction of this complex by evaporative removal of the ammonia leads to the formation of cellulose III, but removal by water exchange results in regeneration of cellulose I. The removal technique alters the physical properties of the treated celluloses as well as its crystal structure. Its impact on the pore size distribution was assessed using the reverse gel permeation chromatography technique with whole fiber columns in an earlier investigation using sterilized medical cotton batting [27]. These purified cotton battings were treated with liquid ammonia, which was removed by volatilization at ambient temperature, by volatilization at elevated temperature, and by water exchange. Results are given in Figure 6. All three liquid ammonia treatments increased the internal pore volumes accessible to small molecules in the purified cotton. The greatest increase was noted when the ammonia was removed by water exchange and the least when volatilization at elevated temperature was employed.

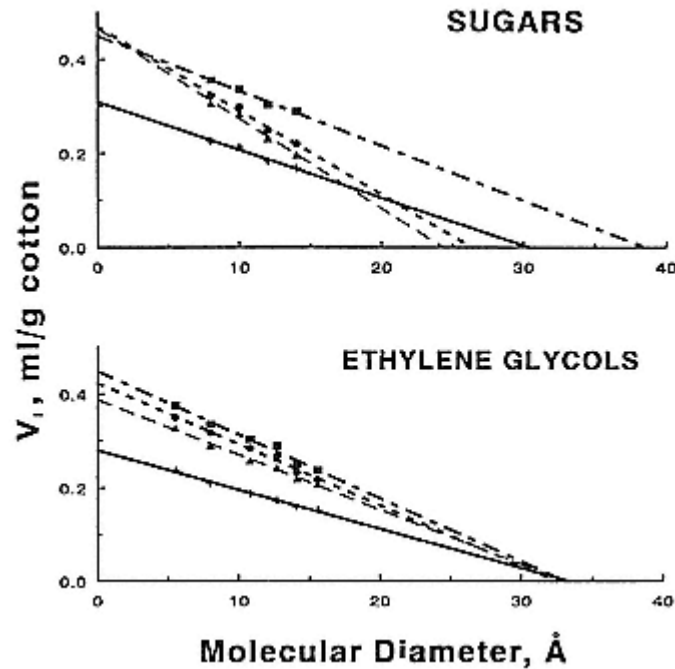


Figure 6
 Internal water (V_i) in purified (+),
 ammonia-96°C (▲),
 ammonia-25°C (●), and
 ammonia—water (■) treated
 cotton battings accessible
 to sugars and ethylene
 glycols.

Ambient temperature volatilization had an intermediate effect. Decreases in the volumes of large pores were effected by ammonia treatment followed by volatilization at ambient and elevated temperature. Water exchange of the ammonia resulted in an increase in the volume of large as well as of the small pores.

D— Cross-Linking

1— Dmdheu

Cotton fabric must be cross-linked to impart the easy care properties required by the consumer. At present cotton fabric is cross-linked not with formaldehyde itself but with formaldehyde derivatives of amides. The most widely used of these is dimethyloldihydroxyethyleneurea (DMDHEU) and its various low formaldehyde release modifications. Cross-linking with DMDHEU enhances resilience but with concomitant losses in strength. A study [28] was conducted to determine if these strength losses were associated with changes in the pore size distributions in the cotton fibers. Cotton printcloth was treated with DMDHEU to five add-on levels.

Magnesium chloride hexahydrate was the cross-linking catalyst. The reverse gel permeation chromatographic technique was used to follow changes in pore size distribution. Columns were prepared by settling water slurries of the Wiley-mill ground cotton as described earlier. The series of oligomeric sugars and ethylene glycols were used as molecular probes. These data are shown in Figure 7. Progressive losses in the accessible internal volume were observed with increasing degree of cross-linking across the entire distribution of pore sizes. Increases in resilience were accompanied by the expected losses in strength, which in turn were associated with decreases in the accessible internal volume of the fibers.

Pores are voids between elementary fibrils or microfibrils. It is generally accepted that cross-linking tends to "fix" the cellulose structure in the state in which it exists during the cross-linking process. The cross-links hold the microfibrillar units in close association, which inhibits swelling. The closeness of the association is a function of the conditions and degree of cross-linking. The effect of reaction conditions has been demonstrated with this pore size distribution

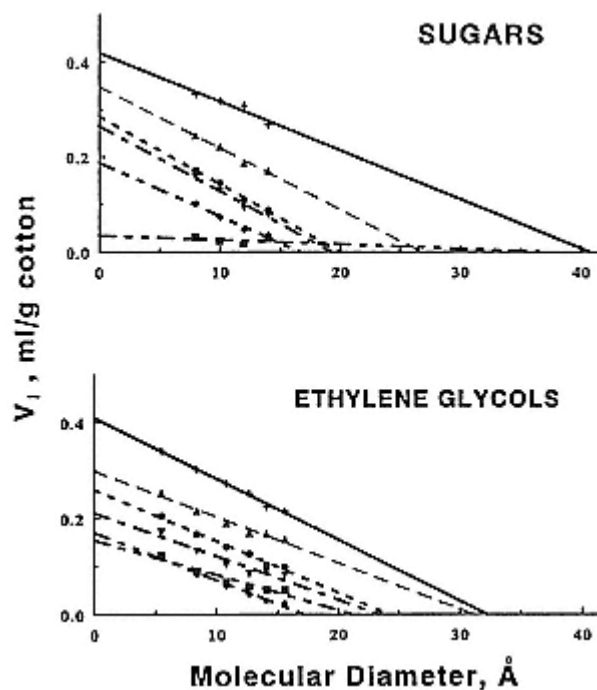


Figure 7
Internal water (V_i) in unmodified cotton
(\times) and cotton cross-linked
with 1% (\blacktriangle), 2%, (\bullet)
4% (\blacktriangledown) 6% (\blacklozenge), and 8%
(\blacksquare) DMDHEU accessible to sugars
and ethylene glycols.

technique for cross-linking with formaldehyde [7]. It was shown that the accessibility of the cotton fiber was increased by reactions with formaldehyde in aqueous solution but decreased when a bake-cure technique was used. DMDHEU was applied in a pad-dry-cure process, which has "fixed" the fibers in the collapsed state that existed when covalent bond formation occurred during curing. The degree to which the cross-linking affected the pore size distribution must be related to the extent of reaction with DMDHEU as the processing conditions were constant. Small, medium, and large pores were comparably affected at the same level of DMDHEU application. Although strength losses were associated with collapse of the internal pore structure of the cotton, they were not associated with the loss of a specific pore size.

2— Dyeability

Cotton that has been cross-linked to impart durable-press properties is intrinsically dye-resistant because of the collapse of the internal structure as described earlier. For this reason cotton fabric is dyed before the cross-linking treatment is applied. Dyeing of textiles in garment form is now of economic interest to the American textile industry. As currently practiced, garments dyed in this manner are made of unmodified cotton and the resulting clothing thus has a rumpled appearance. In order to extend this process to include apparel with durable-press properties, technology had to be developed to overcome the dye-resistant properties of cross-linked cotton.

In the course of an investigation to develop durable-press reagents that do not contain formaldehyde, 4,5-dihydroxy-1,3-dimethyl-2-imidazolidinone (DHDMI) was evaluated as a cross-linking agent for cotton. The treated cotton fabrics, which contained only intralamellar cross-links, differ from conventionally cross-linked cottons, which contain both intra- and interlamellar crosslinks. They proved receptive to direct red 81 but exhibited the more usual dye resistance when larger dye molecules were used (Fig. 8). The internal structure of cotton cross-linked with this reagent was thus of interest.

The reverse gel permeation chromatography technique was employed to assess differences in the pore size distribution (Fig. 9) between cottons cross-linked with DHDMI and with DMDHEU to comparable levels of wrinkle recovery [29]. Results were compared to the receptivity of these cotton samples to the dye direct red 81 (Fig. 10). It was shown that although cross-linking of cotton with either DMDHEU or DHDMI reduced accessible internal volume, those treated with DHDMI retained substantially more accessible internal volume across the entire range of pore sizes. Increasing add-on of DMDHEU further reduced the accessible internal volume. In contrast, the accessible internal volume in DHDMI treated cotton was increased by additional add-on of this reagent. The trends with respect to relative receptivity to direct red 81 generally related better to the quantity of residual large pores (17 Å) than to remaining intermediate pores (10 Å).

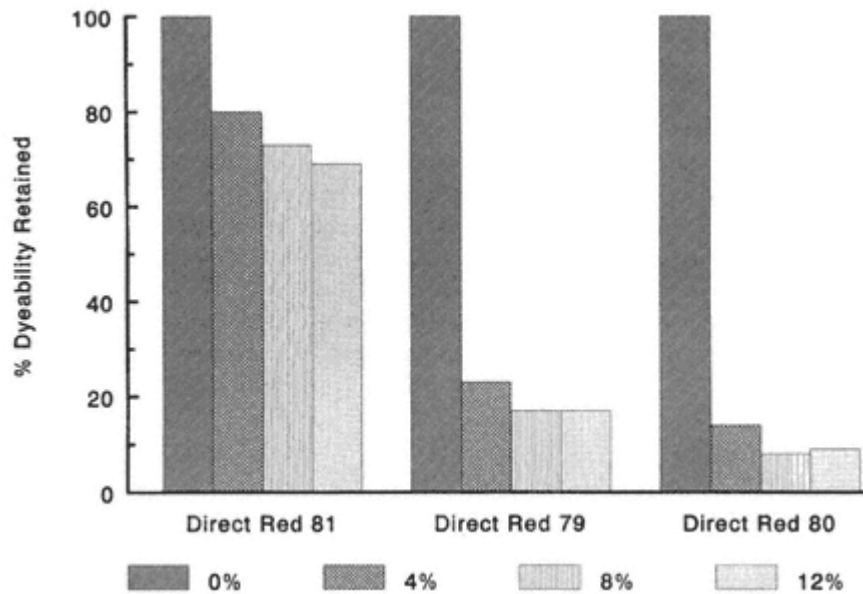


Figure 8
Dyeability with direct red 81 (molecular weight 676),
direct red 79 (molecular weight 1049),
and direct red 80 (molecular weight 1373) after
cross-linking with DHDMI at levels indicated.

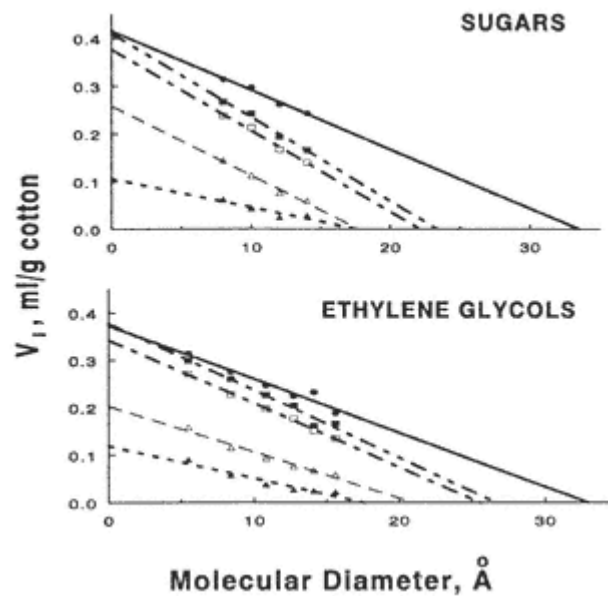


Figure 9
Internal water (V_i) in unmodified cotton
(●) and cotton cross-linked
with 3% DMDHEU (Δ), 8%
DMDHEU (\blacktriangle), 7.5% DHDMI (\square),
and 15% DHDMI (\blacksquare).

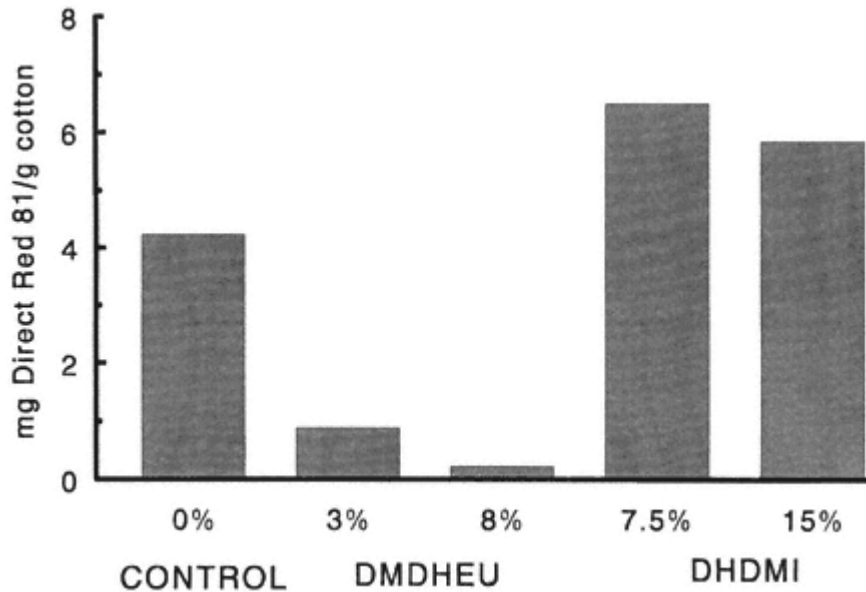


Figure 10
Effect of cross-linking with DMDHEU and DHDMI
on uptake of direct red 81.

3—

Formaldehyde-Free Reagents

OSHA regulations regarding allowable formaldehyde in air in the workplace have prompted research into the development of new cross-linking reagents that do not contain formaldehyde. Several formaldehyde-free cross-linking systems have been developed. The addition product of 1,3-dimethylurea and glyoxal (4,5-dihydroxy-1,3-dimethylimidazolidinone, DHDMI) is available commercially. Glyoxal with either ethylene glycols or 1,6-hexanediol as coreactive additives was another system explored [30, 31]. Systems based on polycarboxylic acids as cross-linking agents for cellulose [32, 33] with catalysis by alkali metal salts of phosphorus containing inorganic acids [34] are an ongoing area of research. The most effective of these organic acids to date is 1,2,3,4-butanetetracarboxylic acid (BTCA).

These formaldehyde-free reagents differ in the weight add-on required to impart easy care performance to cotton fabric. Generally it requires considerably more reagent to impart wrinkle resistance to cotton with the formaldehyde-free reagents than it does with the formaldehyde derivative DMDHEU. This suggests that cross-links imparted by the formaldehyde-free agents differ considerably from those from DMDHEU. A study was conducted to compare the selected formaldehyde-free cross-linking agents among themselves and with the conventional agent DMDHEU with respect to the degree to which they altered the pore size distribution in the crosslinked cotton.

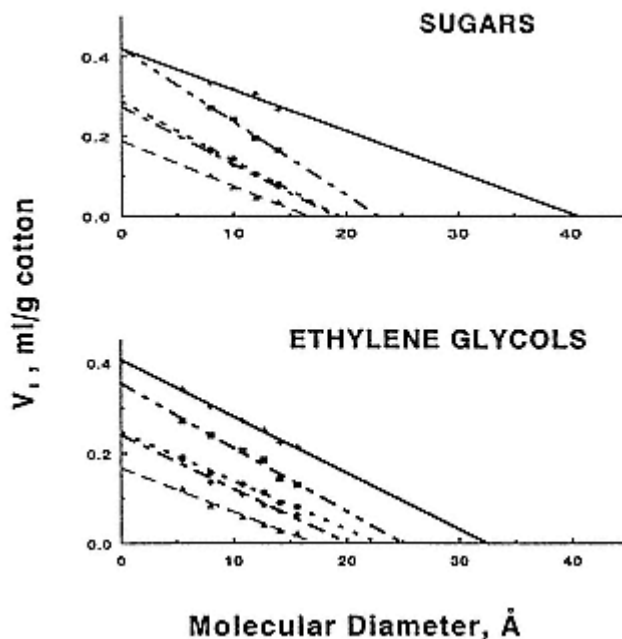


Figure 11
 Internal water (V_i) in unmodified cotton
 (+) and cotton cross-linked
 with DHDMI (■), BTCA (◆),
 glyoxal/glycol (●), and
 DMDHEU (▲).

The formaldehyde-free reagents were BTCA (butanetetracarboxylic acid), DHDMI (dihydroxydimethylimidazolidinone), and the glyoxal/glycol system. The fabric was an 80×80 cotton printcloth. Treatments were designed to impart the same degree of resilience to the fabric as measured by the conditioned wrinkle recovery angle. This was achieved with the exception of DHDMI, where a lower level of resilience was realized. The reverse gel permeation chromatographic technique was used to follow changes in pore size distribution. Columns were prepared by settling water slurries of the Wiley-milled cotton as described earlier. The series of oligomeric sugars and ethylene glycols were used as molecular probes. Results are given in Figure 11. It was concluded that formaldehyde-free cross-linking reagents effect a lower level of collapse of the internal pore structure of the cotton fiber than does DMDHEU at generally comparable levels of resilience.

4— BTCA Catalysts

The key to the success of cross-linking of cellulose with polycarboxylic acids was the development of new catalyst systems based on alkali metal salts of phospho-

rus containing inorganic acids [35, 36]. The most effective of these organic acids to date is 1,2,3,4-butanetetracarboxylic acid (BTCA). The level of textile performance that is realized with BTCA applied to cotton fabric is directly related to the catalyst used. An investigation [37] was therefore conducted in which we evaluated cotton cross-linked with BTCA via catalysis by six alkali metal salts of phosphorus acids and by sodium carbonate. The catalysts included in this study were $\text{NaH}_2\text{PO}_2 \cdot \text{H}_2\text{O}$, $\text{NaH}_2\text{PO}_3 \cdot 2.5\text{H}_2\text{O}$, $\text{Na}_2\text{HPO}_3 \cdot 5\text{H}_2\text{O}$, $\text{NaH}_2\text{PO}_4 \cdot \text{H}_2\text{O}$, Na_2HPO_4 , $\text{Na}_4\text{P}_2\text{O}_7$, and Na_2CO_3 . The treatments were applied to all-cotton printcloth via a pad-dry-cure process. Pore size distribution was assessed on Wiley milled fabric via the reverse gel permeation chromatographic technique. The water-soluble molecular probes employed were sugars and ethylene glycols. Plots of V_i against molecular diameter are given in Figure 12, and a comparison of the effects on small and medium sized pores is given in Figure 13. Definite patterns were observed in textile performance realized with the different catalysts. It was shown that the total volume in residual small pores was inversely related to the resilience level achieved and that retained breaking strength was directly related to the volume in

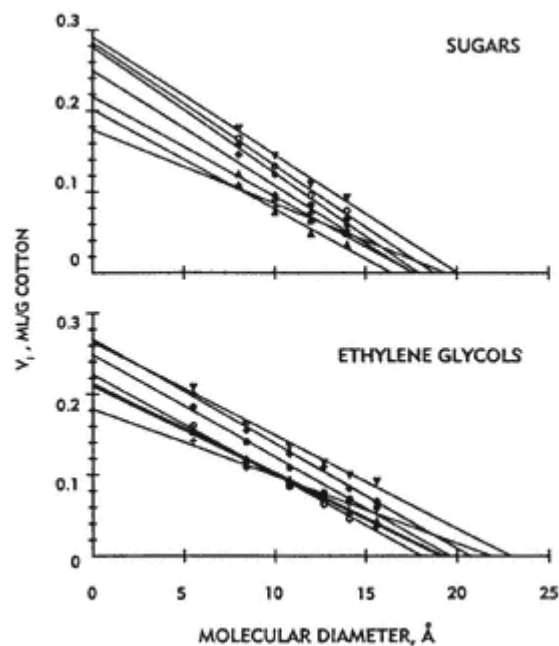


Figure 12
Internal water (V_i) in cotton cross-linked with BTCA via Na_2HPO_2 (+), NaH_2PO_3 (▲), Na_2HPO_3 (+), NaH_2PO_4 (Δ), Na_2HPO_4 (O), $\text{Na}_4\text{P}_2\text{O}_7$ (●), and Na_2CO_3 (V) catalysis as functions of the molecular diameters of sugars and ethylene glycols.

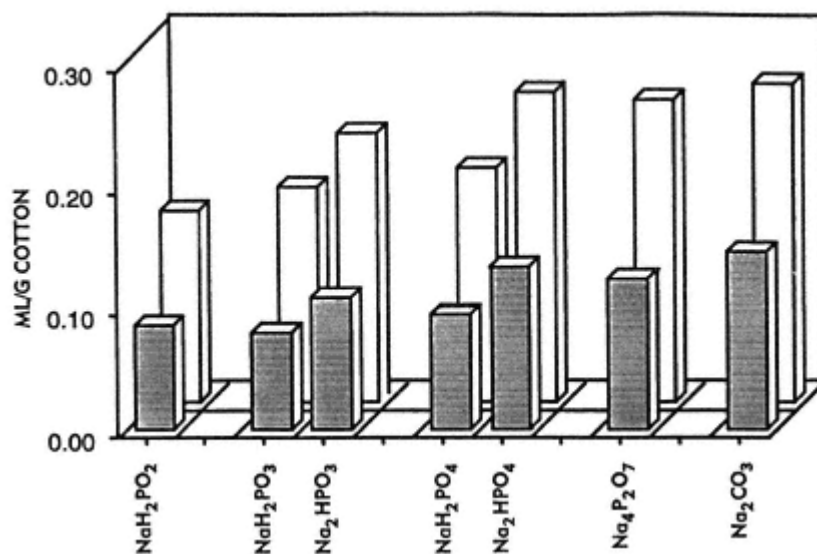


Figure 13
Comparison of residual small (V_2 , open bars)
and medium (V_{10} , hatched bars) pores
in cotton cross-linked with BTCA; sugars
were used as molecular probes.

residual small pores. Patterns with respect to abrasion resistance were more complex. As BTCA add-ons were comparable, the data suggest that the more effective catalysts, NaH_2PO_2 and NaH_2PO_3 , are either effecting a greater number of crosslinks in the cotton or producing cross-links that differ in actual structure.

V—

Future Work

Research in this area continues. It is being used to study differences in accessibility of different cross-linking agents for cotton to the interior of the cotton fibers. Work is also being initiated into changes in the pore size distribution effected by treatment with cellulase enzymes, which is now a commercial practice.

References

1. J. Porath and P. Flodin, Gel filtration: A method for desalting and group separation, *Nature* 183:1657 (1959).
2. L.G. Aggebrandt and O. Samuelson, Penetration of water-soluble polymers into cellulose fibers, *J. Appl. Polym. Sci.* 8:2801 (1964).
3. J. E. Stone and A. M. Scallan, A structural model for the cell wall of water swollen wood pulp fibres based on their accessibility to macromolecules, *Cellulose Chem. Technol.* 2:343 (1968).

4. L. F. Martin and S. P. Rowland, Gel permeation properties of decrystallized cotton cellulose, *J. Chromatogr.* 28:139 (1967).
5. L. F. Martin and S. P. Rowland, Gel permeation properties of cellulose. I. Preliminary comparison of unmodified and crosslinked, decrystallized cotton cellulose, *J. Polym. Sci. Part A-1* 5:2563 (1967).
6. L. F. Martin, F. A. Blouin, N. R. Bertoniére, and S. P. Rowland, Gel permeation technique for characterizing chemically modified celluloses, *Tappi* 52:708 (1969).
7. L. F. Martin, N. R. Bertoniére, F. A. Blouin, M. A. Brannan, and S. P. Rowland, Gel permeation properties of cellulose II: Comparison of structures of decrystallized cotton crosslinked with formaldehyde by various processes, *Textile Res. J.* 40:8 (1970).
8. L. F. Martin, F. A. Blouin, and S. P. Rowland, Characterization of the internal pore structures of cotton and chemically modified cottons by gel permeation, *Separation Sci.* 6:287 (1971).
9. N. R. Bertoniére, L. F. Martin, and S. P. Rowland, Stereoselectivity in the elution of sugars from columns of Sephadex G15, *Carbohydrate Res.* 19:189 (1971).
10. L. F. Martin, N. R. Bertoniére, and S. P. Rowland, The effects of sorption and molecular size of solutes upon elution from polyhydroxylic gels, *J. Chromatogr.* 64:263 (1972).
11. S. P. Rowland and N. R. Bertoniére, Some interactions of water-soluble solutes with cellulose and Sephadex, *Textile Res. J.* 46:770 (1976).
12. F. A. Blouin, L. F. Martin, and S. P. Rowland, Gel-permeation properties of cellulose. Part III: Measurement of pore structure of unmodified and of mercerized cottons in fibrous form, *Textile Res. J.* 40:809 (1970).
13. F. A. Blouin, L. F. Martin, and S. P. Rowland, Gel-permeation properties of cellulose. Part IV: Changes in pore structure of fibrous cotton produced by crosslinking with formaldehyde, *Textile Res. J.* 40:959 (1970).
14. C. P. Wade, Preparation of whole-fiber cotton gel-filtration chromatography columns, *J. Chromatogr.* 268:187 (1983).
15. S. P. Rowland, C. P. Wade, and N. R. Bertoniére, Pore structure analysis of purified, sodium hydroxide-treated and liquid ammonia-treated cotton celluloses, *J. Appl. Polym. Sci.* 29:3349 (1984).
16. K. Bredereck and A. Blüher, Determination of the pore structure of cellulose fibers by exclusion chromatography. Principles and use examples for swelling treatments and resin finishing of cotton fabrics, *Melliand Textilberichte* 73:297(English), 652 (German) (1992).
17. C. M. Ladisch, Y. Yang, A. Velayudhan, and M. R. Ladisch, A new approach to the study of textile properties with liquid chromatography—Comparison of void volume and surface area of cotton and ramie using a rolled fabric stationary phase, *Textile Res. J.* 62:361 (1992).
18. C. M. Ladisch and Y. Yang, A new approach to the study of textile dyeing properties with liquid chromatography—Part I: Direct dye absorption on cotton using a rolled fabric stationary phase, *Textile Res. J.* 62:481 (1992).
19. Y. Yang and C. M. Ladisch, A new approach to the study of textile dyeing properties with liquid chromatography—Part II: Compatibility of basic dyes for acrylic fabric, *Textile Res. J.* 62:531

(1992).

20. R. Nelson and D. W. Oliver, Study of cellulose and its relation to reactivity, *J. Polym. Sci. Part C* 36:305 (1968).
21. P. H. Hermans, *Physics and Chemistry of Cellulose Fibers with Particular Reference to Rayon*, Elsevier, New York, 1949, p 20.
22. N. R. Bertoniére, W. D. King, and S. E. Hugh's, Effect of variety on the pore structure of the cotton fiber, *Lignocellulosics—Science, Technology, Development and Use* (J. F. Kennedy, G. O. Phillips, and P. A. Williams, eds.), Ellis Horwood Limited, Chichester, UK, 1992, p. 457.
23. H. M. Welo, H. M. Ziffle, and A. W. McDonald, Swelling capacities of fibers. Part II: Centrifuge studies, *Textile Res. J.* 22:261 (1952).
24. N. R. Bertoniére, S. P. Rowland, M. Kabir, and A. Rahman, Gel permeation characteristics of jute and cotton, *Textile Res. J.* 54:434 (1984).
25. N. R. Bertoniére and W. D. King, Effect of scouring/bleaching, caustic mercerization and liquid ammonia treatment on the pore structure of cotton textile fibers, *Textile Res. J.* 59:114 (1989).
26. N. R. Bertoniére, Pore structure analysis of cotton cellulose via gel permeation chromatography, *Cellulose—Structure and Functional Aspects* (J. F. Kennedy, G. O. Phillips and P. A. Williams, eds.), Ellis Horwood Limited, Chichester, United Kingdom, 1989, p. 99.
27. N. R. Bertoniére, W. D. King, and S. P. Rowland, Effect of mode of agent removal on the pore structure of liquid ammonia treated cotton cellulose, *J. Appl. Polym. Sci.* 31:2769 (1986).
28. N. R. Bertoniére and W. D. King, Residual pore volume, resilience and strength of crosslinked cotton cellulose, *Textile Res. J.* 60:606 (1990).
29. N. R. Bertoniére and W. D. King, Pore structure and dyeability of cotton crosslinked with DMDHEU and with DHDMI, *Textile Res. J.* 59:608 (1989).
30. C. M. Welch, Formaldehyde-free durable press finishing of cotton, *Textile Chem. Color.* 16:265 (1984).
31. C. M. Welch and J. G. Peters, Low, medium, and high temperature catalysts for formaldehyde-free durable press finishing by the glyoxal-glycol process, *Textile Res. J.* 57:351 (1987).
32. S. P. Rowland, C. M. Welch, M. A. F. Brannan, and D. M. Gallagher, Introduction of ester cross links into cotton cellulose by a rapid curing process, *Textile Res. J.* 37:933 (1967).
33. S. P. Rowland, C. M. Welch, and M. A. F. Brannan, Cellulose fiber crosslinked and esterified with polycarboxylic acids, U. S. Patent 3,526,048, September 1, 1970.
34. C. M. Welch and B. K. Andrews, Catalysis for processes for formaldehyde-free durable press finishing of cotton textiles with polycarboxylic acids, U. S. Patent 4,820,307, April 11, 1989.
35. C. M. Welch, Tetracarboxylic acids as formaldehyde-free finishing agents. Part I: Catalyst, additive, and durability studies, *Textile Res. J.* 58:480 (1988).
36. C. M. Welch, Durable press finishing without formaldehyde, *Textile Chem. Color* 22:13 (1990).
37. N. R. Bertoniére, W. D. King, and C. M. Welch, Effect of catalyst on the pore structure of cotton cellulose cross-linked with butanetetracarboxylic acid, *Textile Res. J.* 64:247–255 (1994)

8—**Pore Structure in Fibrous Networks as Related to Absorption**

Ludwig Rebenfeld, Bernard Miller, and Ilya Tyomkin
TRI/Princeton, Princeton, New Jersey

I—**Introduction**

The textile production process is remarkably flexible, allowing the manufacture of fibrous materials with widely diverse physical properties. All textiles are discontinuous materials in that they are produced from macroscopic subelements (finitelength fibers or continuous filaments). In woven and knitted textiles, the fibers or filaments are first formed into spun or multifilament yarns prior to either weaving or knitting. In nonwoven materials, the fibers or filaments are processed directly into the final planar structure, and then either chemically or physically bonded or mechanically interlocked. The chemical, physical, and mechanical properties of textile materials depend on the inherent properties of the component fibers and on the geometric arrangement of the fibers in the structure.

The discontinuous nature of textile materials means that they have void spaces or pores that contribute directly to some of the key properties of textiles, for example, thermal insulating characteristics, liquid absorption properties, and softness and other tactile characteristics. In physical terms, textile materials have solidifies less than unity and therefore finite porosities. This chapter considers the evaluation of the pore structure of textile materials, particularly as that structure relates to liquid absorption and to the porous barrier characteristics of these and related planar materials.

II—**Porosity****A—*****Basic Concepts***

Porosity is one of the important physical quantities that is used to describe textile materials. Porosity, ϵ , represents the fraction of the nominal bulk volume of a ma-

terial that is occupied by void space. In terms of textile properties, it can be expressed as

$$\epsilon = 1 - \frac{W}{dh} \quad (1)$$

where W is the areal density (mass per unit area) of the fabric, h is its nominal thickness, and d is the bulk density of the fibers from which the fabric is produced. Porosity can range widely, depending on product design and processing techniques.

The cross-sectional shapes of natural and man-made textile fibers vary widely, and the pore structure of a fiber assembly is strongly influenced by this geometrical characteristic. The manner in which fibers can pack in an assembly is largely determined by their cross-sectional shape. If we model fibers as being circular in cross section, then the packing of uniform cylinders provides a good example of how this factor limits the lowest porosity that can be achieved. The closest possible packing of parallel cylinders with uniform radii is in rhombohedral (hexagonal) packing, shown schematically in two dimensions in Figure 1. The porosity of such a system is 0.093, which is the minimum possible value of porosity for cylinders of equal radii. This value is independent of the cylinder radius. To the extent that this model represents an idealized two-dimensional textile material composed of identical fibers with circular cross-sectional shapes, the lowest possible porosity of a textile material is 0.093. If the fibers were not all equal in radius or if they deviated from being perfectly circular in cross-sectional shape, the minimum porosity would increase significantly. On the other hand, if the fibers were square or rectangular in cross-sectional shape, the porosity of the closest packed structure

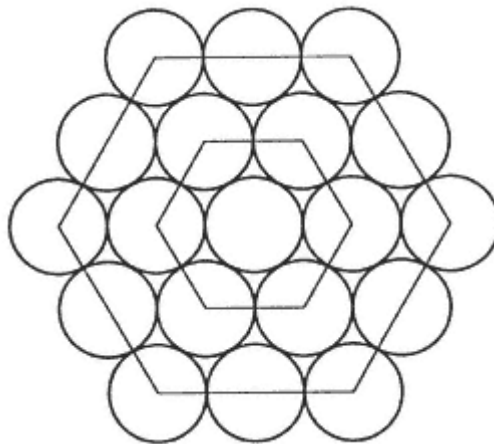


Figure 1
Two-dimensional representation of
close-packed cylinders of equal
and uniform radii.

could approach zero. In contrast to cylinders, the closest rhombohedral packing of spheres with uniform radii would produce a porosity of 0.259 [1].

The porosities of real textile materials are surprisingly high, reflecting the fact that the component fibers are not densely packed and that the fibers are not uniform in shape and diameter. In fact, textile materials are normally designed to have relatively high porosities. Open and bulky woven and knitted fabrics and certain airlaid nonwovens have porosities in the range of 0.95 and higher. Even those fabrics that appear dense and solid will have porosities in the range of 0.6 to 0.7. Porosity is an especially important property in connection with those textile materials that are used as liquid absorption media. Absorption can be defined as the process wherein liquid displaces the air in the void spaces or the pores in the material, either spontaneously as in wicking or under an external driving pressure. The amount of liquid that can be absorbed is a direct function of the fabric porosity.

The porosity of a material can be experimentally determined by a number of methods, including those based on direct gravimetric and volumetric measurements, optical techniques, liquid imbibition, and gas expansion [2,3]. For textile materials, direct gravimetric and volumetric measurements are normally used to obtain the quantities required in Eq. (1). In quantifying porosity, it is important to distinguish between porosity values that are based on pores that are effective and those that are isolated. Effective pores are defined as those that form a continuous and interconnected phase that reaches to the nominal surface of the network. Isolated pores, on the other hand, are completely enclosed by the solid material and are not a part of the continuous phase. Obviously, only the effective interconnected pores contribute to the sorptive capacity of a material. Direct measurements and optical techniques provide estimates of the total porosity of a material, while imbibition measurements provide estimates of porosities based only on the effective interconnected pores.

B—

Porosity and Compression

The porosity of a textile material is strongly affected by lateral compressive forces to which the material is subjected. This is due to the fact that textiles are highly porous and therefore compliant, as shown in Figure 2, where the thickness of three glass-fiber nonwovens differing in areal density is plotted as a function of compressive pressure [4]. The thickness of each of these materials decreases rapidly at first and then levels off with increasing pressure. These results also indicate that the compressed thickness depends on the areal density of the material; that is, at a given compressive pressure the thickness increases with the areal density. Calculating the porosities of the three nonwovens at each compressive pressure, the relationship shown in Figure 3 is obtained. The data for the three materials fall on the same line, indicating that fabrics with different areal densities may not compress to the same thickness, but they do compress to the same porosity. It is also

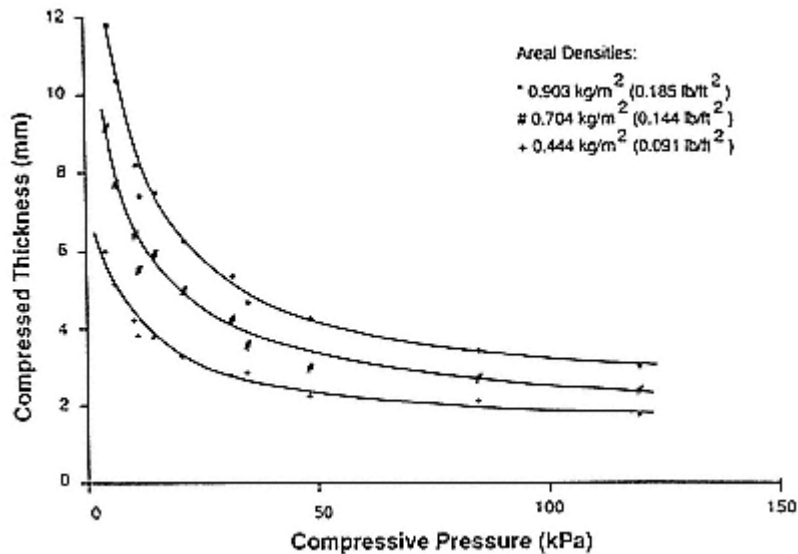


Figure 2
 Thickness of three glass fiber mats as a function
 of compressive pressure.
 (From Ref. 4.)

interesting to note the strong dependence of porosity on low levels of compressive pressure, and the apparent leveling off of porosity with increasing compressive pressure. Beyond a certain level of compressive pressure, the fibers in the nonwoven become so tightly packed that further pressure cannot cause a further decrease in fabric thickness since the fibers themselves must be considered incompressible. The exact relationships between fabric areal density, thickness, porosity, and compressive pressure, and the shape of curves such as those shown in Figures 2 and 3, will depend on the type of fiber used, the fiber cross-sectional shape and dimensions, and the structure of the material, that is, whether it is a woven or knitted fabric or a specific type of nonwoven material. Nevertheless, the porosities of all textile materials are strongly dependent on compressive pressure. This is particularly important in understanding the pressure dependence of the liquid absorption characteristics of textiles.

It must be emphasized that porosity is an average property of a fibrous material that describes the structure of the material in a very limited way. It provides no description or information about the nature of the void space or about the structure of the fiber network. Entirely different materials can have the same porosity values, and we must look for other means of describing and quantifying the pore structure of textile materials.

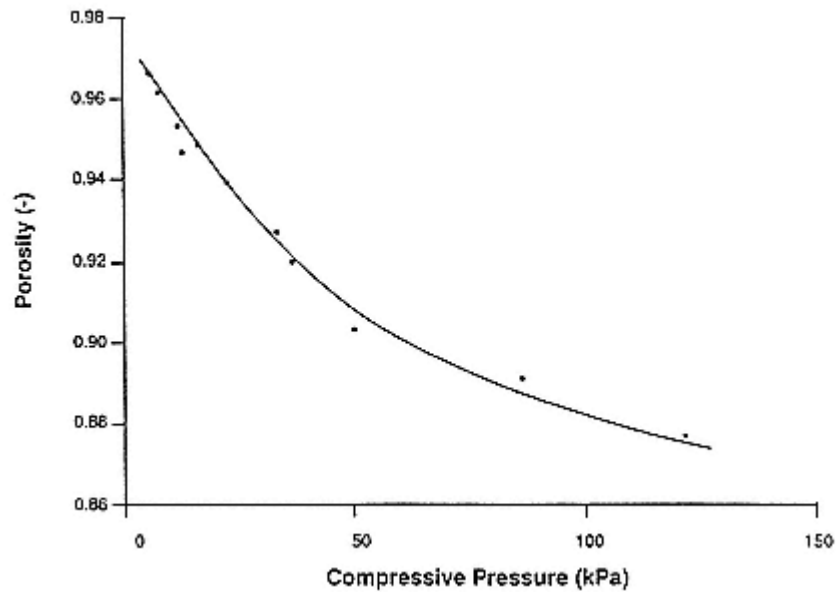


Figure 3
Porosity of glass fiber mats as a function of
compressive pressure.
(From Ref. 4.)

III— Pore Structure

A— *Pore Dimensions*

While porosity is an important physical quantity, a more descriptive way of characterizing the porous nature of a network is by quantifying the dimensions of the pores. Considering the pore shape shown in Figure 4, pore dimensions can be described in many terms, for example, their volumes, surface areas, average diameters, and minimum diameters, frequently referred to as pore throats. Each of these dimensions could be critical in controlling a specific kind of behavior. Pore volume is the dominant factor that determines the capacity for absorption of liquid. The total surface area would be the critical property if adsorption phenomena were of primary interest. Pore throat dimensions would be most important if one were concerned with porous barriers and flow-through processes (e.g., filtration), where particle capture and resistance to liquid flow would be directly related to the size of these throats. Entrance or exit pore dimensions (end diameters) would be crucial in predicting the probability of particulates penetrating and being retained by the interior of a structure. An average pore diameter could be used as a general characterization of a porous network.

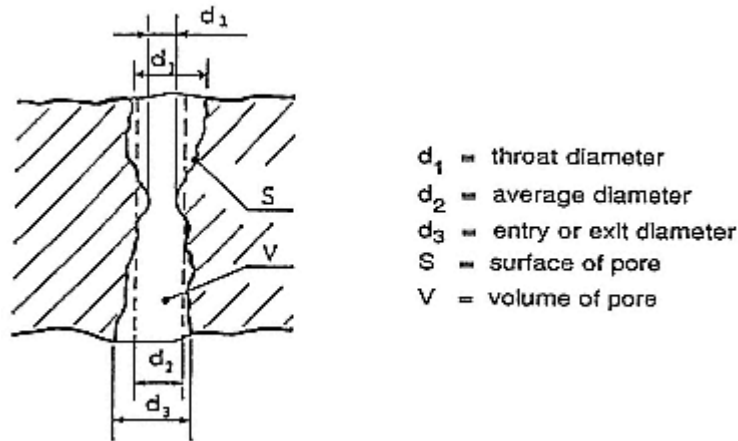


Figure 4
Schematic of a pore in a fibrous network.

In addition to the characterization of pore dimensions on the basis of geometrical considerations, pore dimensions can be quantified on the basis of various permeability models. For example, the Carman—Kozeny flow model yields a hydraulic radius that is related to the volume-to-surface ratio of a pore or capillary. Discussion of permeability models is outside the scope of this chapter, and the reader is referred to standard texts on this subject [2,3].

B—

Distribution of Pore Sizes

While average values of geometric quantities describing pore dimensions provide valuable information about network structure, they are only a little more informative than average porosity values. Fibrous networks are invariably heteroporous (i.e., the dimensions of the pores are not equal), and it is therefore important to consider the distribution of these quantities. Depending on product design and the processing technologies, pore size distributions can be broad or narrow, unimodal, bimodal, or even trimodal.

Pore size distributions in nonwovens are typically unimodal and relatively broad, with a range of values that may cover several orders of magnitude. Nonwovens with bi- and trimodal distributions can also be produced. Woven fabrics manufactured from continuous monofilaments, sometimes referred to as screening fabrics, have pore dimensions that are essentially monodisperse. The pores in such fabrics are those formed between the monofilaments and at monofilament crossover points, and their dimensions are determined by the filament diameters and the weave pattern.

Woven fabrics manufactured from spun or multifilament yarns have bimodal pore size distributions. A system of large pores is formed by the interlacing yarns as determined by the weave pattern, just as in the case of monofilament woven fabrics. These interyarn pores may be relatively uniform in size and shape. However, another system of pores is formed within the yarn structure between the component fibers or filaments. These intrayarn or interfiber pores are much smaller than the interyarn pores and are in most cases somewhat more polydisperse. Their size and shape are determined by the fiber or filament diameters and cross-sectional shapes, and by the degree of twist that is imposed to impart yarn cohesion and mechanical integrity.

C—

Liquid Porosimetry

Liquid porosimetry, also referred to as liquid porometry, is a general term to describe procedures for the evaluation of the distribution of pore dimensions in a porous material based on the use of liquids. There are many forms of liquid porosimetry, but we restrict our discussion to two major methods that are designed to characterize the pore structure in terms of pore volumes and in terms of pore throat dimensions. Both pore volumes and pore throat dimensions are important quantities in connection with the use of fiber networks as absorption and barrier media. Pore volumes determine the capacity of a network to absorb liquid, that is, the total liquid uptake. Pore throat dimensions, on the other hand, are related to the rate of liquid uptake and to the barrier characteristics of a network.

IV—

Pore Volume Distribution Analysis

A—

Basic Concepts

Liquid porosimetry evaluates pore volume distributions (PVD) by measuring the volume of liquid located in different size pores of a porous structure. Each pore is sized according to its effective radius, and the contribution of each pore size to the total free volume of the porous network is determined. The effective radius R of any pore is defined by the Laplace equation:

$$R = \frac{2\gamma \cos \theta}{\Delta P} \quad (2)$$

where

γ = liquid surface tension

θ = advancing or receding contact angle of the liquid

ΔP = pressure difference across the liquid/air meniscus

For liquid to enter or drain from a pore, an external gas pressure must be applied that is just enough to overcome the Laplace pressure ΔP .

In the case of a dry heteroporous network, as the external gas pressure is decreased, either continuously or in steps, pores that have capillary pressures lower than the given gas pressure ΔP will fill with liquid. This is referred to as liquid intrusion porosimetry and requires knowledge of the advancing liquid contact angle. In the case of a liquid-saturated heteroporous network, as the external gas pressure is increased, liquid will drain from those pores whose capillary pressure corresponds to the given gas pressure ΔP . This is referred to as liquid extrusion porosimetry and requires knowledge of the receding liquid contact angle. In both cases, the distribution of pore volumes is based on measuring the incremental volume of liquid that either enters a dry network or drains from a saturated network at each increment of pressure.

B—

Instrumentation

Until recently, the only version of this type of analysis to evaluate PVDs in general use was mercury porosimetry [5]. Mercury was chosen as the liquid because of its very high surface tension so that it would not be able to penetrate any pore without the imposition of considerable external pressure. For example, to force mercury into a pore 5 μm in radius requires a pressure increase of about 2 atm. While this might not be a problem with hard and rigid networks, such as stone, sand structures, and ceramics, it makes the procedure unsuitable for use with fiber materials that would be distorted by such compressive loading. Furthermore, mercury intrusion porosimetry is best suited for pore dimensions less than 5 μm , while important pores in typical textile structures may be as large as 1000 μm . Some of the other limitations of mercury porosimetry have been discussed by Winslow [6] and by Good [7].

A more general version of liquid porosimetry for PVD analysis, particularly well suited for textiles and other compressible planar materials, has been developed by Miller and Tyomkin [8]. The underlying concept was earlier demonstrated for low-density webs and pads by Burgeni and Kapur [9]. Any stable liquid of relatively low viscosity that has a known $\cos \theta > 0$ can be used. In the extrusion mode, the receding contact angle is the appropriate term in the Laplace equation, while in the intrusion mode the advancing contact angle must be used. There are many advantages to using different liquids with a given material, not the least of which is the fact that liquids can be chosen that relate to a particular end use of a material.

The basic arrangement for liquid extrusion porosimetry is shown in Figure 5. In the case of liquid extrusion, a presaturated specimen is placed on a microporous membrane, which is itself supported by a rigid porous plate. The gas pressure within the closed chamber is increased in steps, causing liquid to flow out of some of the pores, largest ones first. The amount of liquid removed at each pressure level

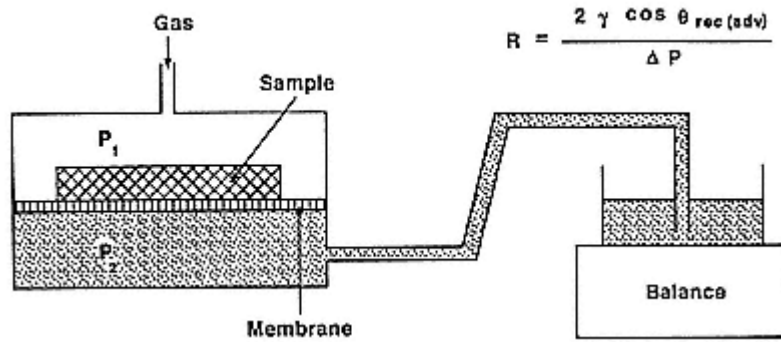


Figure 5
Basic arrangement for liquid porosimetry to quantify pore volume distributions.
(From Ref. 10.)

is monitored by the top-loading recording balance. In this way, each incremental change in pressure (corresponding to a pore size according to the Laplace equation) is related to an increment of liquid mass. To induce stepwise drainage from large pores requires very small increases in pressure over a narrow range that are only slightly above atmospheric pressure, whereas to analyze for small pores the pressure changes must be quite large. These requirements are illustrated in Figure 6. In early versions of instrumentation for liquid extrusion porosimetry, pressurization of the specimen chamber was accomplished either by hydrostatic head changes or by means of a single-stroke pump that injected discrete drops of liquid into a free volume space that included the chamber [8]. In the most recent instrumentation developed by Miller and Tyomkin [10], the chamber is pressurized by means of a computer-controlled, reversible, motor-driven piston/cylinder arrangement that can produce the required changes in pressure to cover a pore radius range from 1 to 1000 μm . The pressure is monitored by one of two transducers (a pair is used to maintain sufficient accuracy at both low and high pressures), and the signal is fed to the computer, which, through feedback logic, adjusts the piston position to set the target pressure almost instantly. A schematic of the complete assembly is shown in Figure 7.

The computer also monitors the output of the balance according to a program that identifies when the weight-change rate at a given pressure, corresponding to a given radius, has dropped to an insignificant level. It then activates the instrumentation to reach the next step in the pressurizing sequence, as the number and magnitude of the pressure changes have been programmed as desired beforehand. After drainage at the final pressure level is complete, the instrument can act in reverse to perform a set of liquid intrusions. Multiple drainage/uptake cycles can be programmed to run automatically on the same specimen.

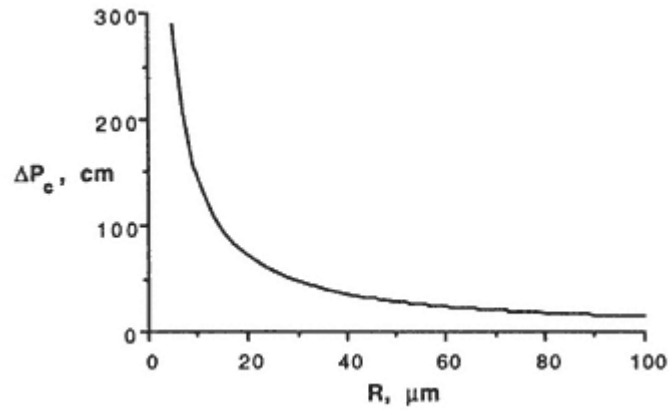


Figure 6
 General form of relationship for water
 between pore size and capillary
 pressure necessary to either fill
 or drain that size pore.
 (From Ref. 10.)

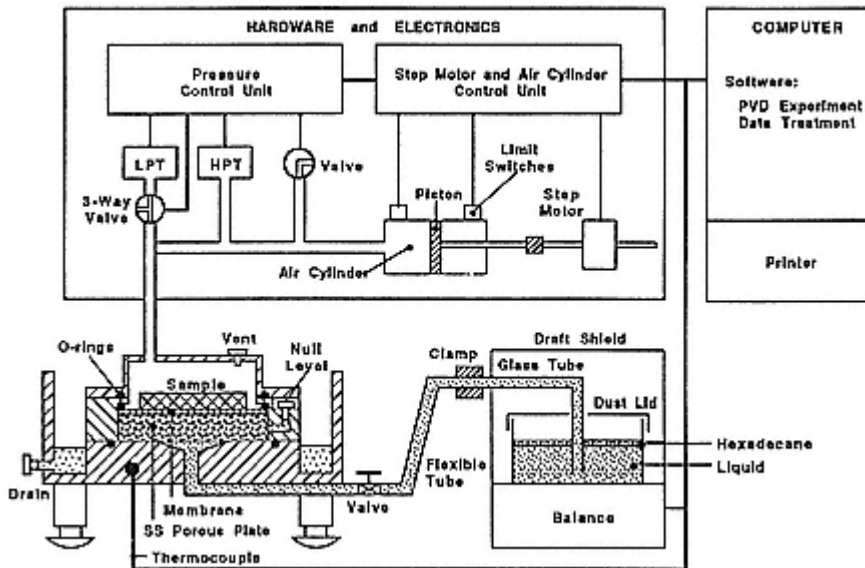


Figure 7
 Schematic of the TRI Autoporosimeter or determining pore volume distributions.
 (From Ref. 10.)

C—

Data Analysis and Applications

Prototype data output for a single cycle incremental liquid extrusion run is shown in Figure 8. The experiment starts from the right as the pressure is increased, draining liquid first from the largest pores. The cumulative curve represents the amount of liquid remaining in the pores of the material at any given level of pressure. The first derivative of this cumulative curve as a function of pore size becomes the pore volume distribution, showing the fraction of the free volume of the material made up of pores of each indicated size.

PVD curves for two typical fabrics woven from spun yarns are shown in Figure 9. The bimodal nature of these curves, discussed previously, is evident. PVD curves for several nonwoven materials are shown in Figure 10. These materials normally have unimodal PVD curves, but generally the pores are larger than those associated with typical woven fabrics. PVD curves for one of the glass fiber nonwovens described in Figure 2 are shown in Figure 11 at three different levels of compression corresponding to the mat thicknesses indicated. Several interesting points can be noted. First, the pore volumes become smaller with increasing compression (decreasing mat thickness), and at the same time the structures appear to have become less heteroporous; that is, the breadth of the PVD curves decreases with increasing compression. Also, the total pore volume (area under each curve), and therefore the sorptive capacity, decreases with compression. Since in many end-use applications fibrous materials are used under some level of compression,

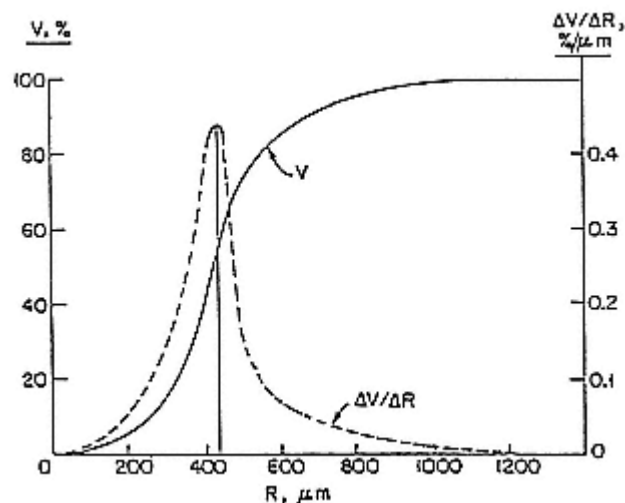


Figure 8
 Prototype data output for a liquid extrusion
 experiment: measured cumulative
 volume and the corresponding
 first derivative, which is the PVD curve.
 (From Ref. 10.)

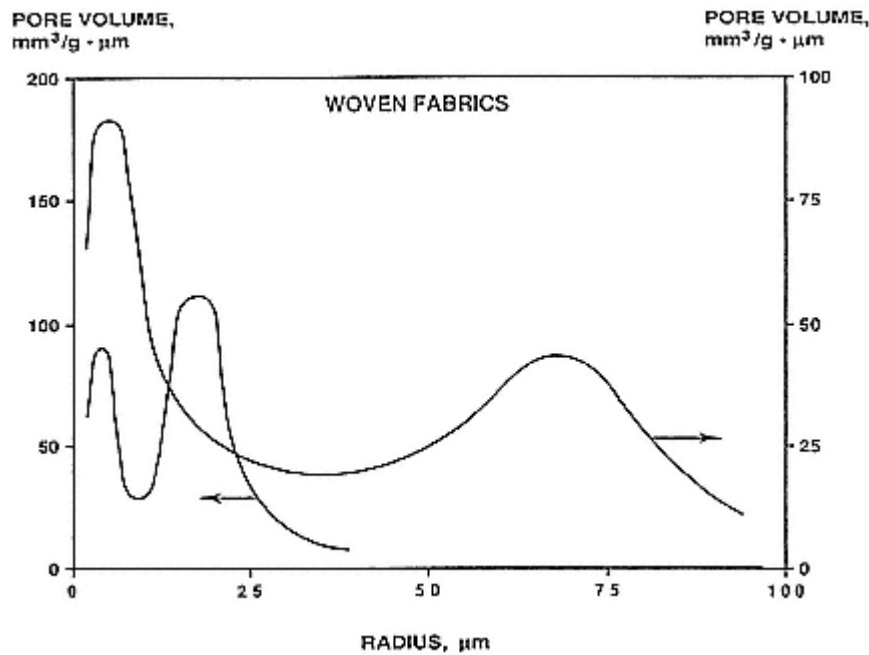


Figure 9
PVD curves for two typical spun yarn woven fabrics.
(From Ref. 10.)

it is particularly important to evaluate pore structure under appropriate compression conditions.

The PVD instrumentation described here, referred to as the TRI Autoporosimeter, is extremely versatile and can be used with just about any porous material, including textiles, paper products, membrane filters, particulates, and rigid foams. It also allows quantification of interlayer pores, surface pores, absorption/desorption hysteresis, uptake and retention capillary pressures, and effective contact angles in porous networks [10]. The technique has also been used to quantify pore volume dimensions and sorptive capacity of artificial skin in relation to processing conditions [11].

V— Pore Throat Analysis

A— *Basic Concepts*

Knowledge of the minimum diameters of continuous or connected pores, commonly referred to as pore throats, is important for many types of applications of porous media. These dimensions of pores are critical in various porous barriers and

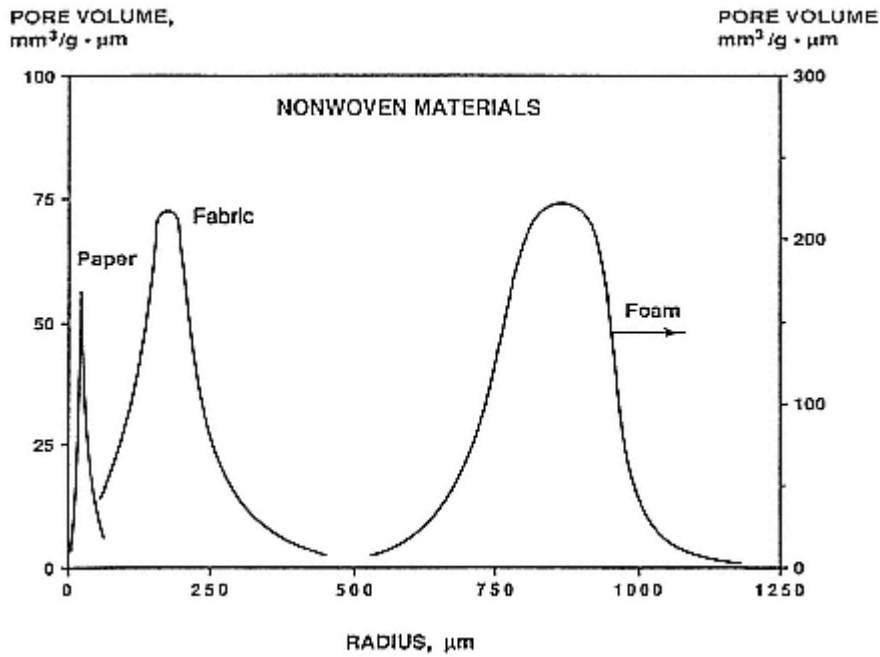


Figure 10
PVD curves for some nonwoven fabrics.
(From Ref. 10.)

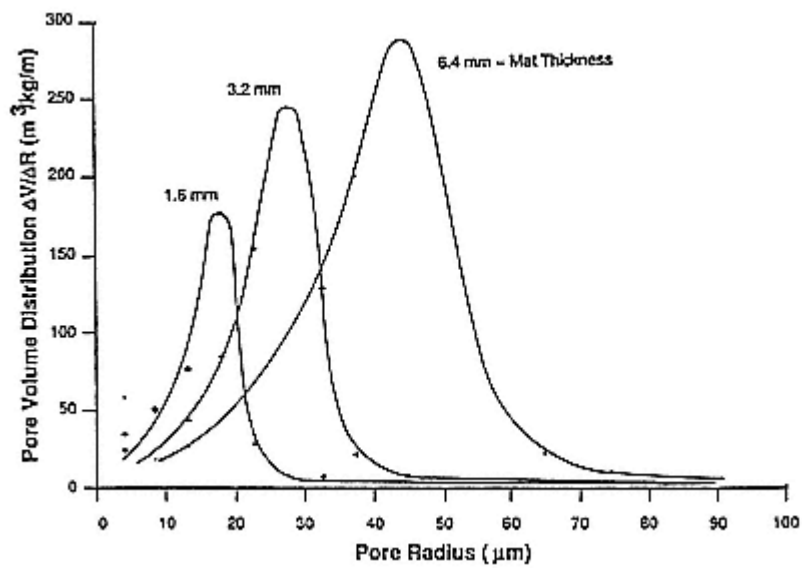


Figure 11
PVD curves for one of the glass fiber mats
described in Fig. 2
at three levels of thickness.
(From Ref. 4.)

flow-through phenomena, for example, in the use of fabrics as filtration media and in several geotextile applications. In terms of absorption media, pore throat dimensions are not related to sorption capacity, but they do play a role in controlling rates of liquid uptake.

The method used to quantify pore throat dimensions is based on the wellknown "minimum bubble pressure" principle, which is operative when gas pressure is applied to one side of a wetted fabric while the other side is in contact with a liquid [12]. As the applied pressure is increased, a critical pressure is reached when the first gas (typically air) bubble emerges through the largest pore available within the sample. This is illustrated schematically in Figure 12. The effective radius of this largest pore is obtained based on Eq. (2), using a liquid with a receding contact angle close to 0° , so that

$$R_{\max} = \frac{2\gamma}{\Delta P} \quad (3)$$

where ΔP is the pressure gradient across the liquid/gas interface.

A single bubble pressure experiment identifies only the largest pore within a scanned area of the material. However, if the specimen were cut into smaller parts, as shown schematically in Figure 13, and each part were characterized separately, then the collected data would present the largest pore in every subpart and would provide the necessary information to construct a pore throat distribution. Small pores have little chance of being detected until the scanned areas become small enough.

B— Instrumentation

Miller et al. [12] designed a multiport chamber shown schematically in Figure 14 to carry out bubble pressure measurements over different wetted areas. Six sets of six holes with different cross-sectional areas were drilled vertically through the

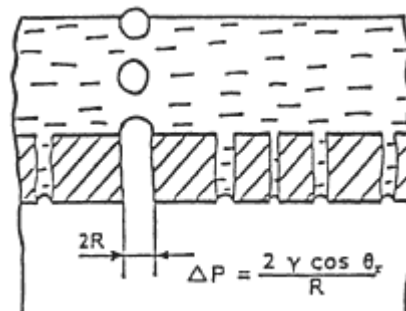


Figure 12
Principle of the minimum bubble
pressure experiment.
(From Ref. 12.)

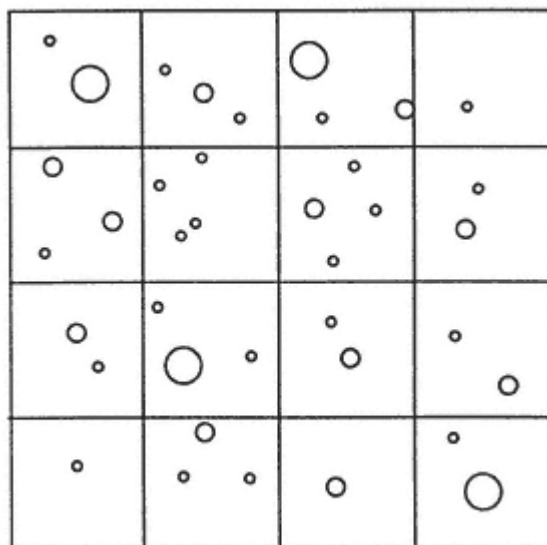


Figure 13
Hypothetical distribution of large pores in a
fibrous network. (From Ref. 12.)

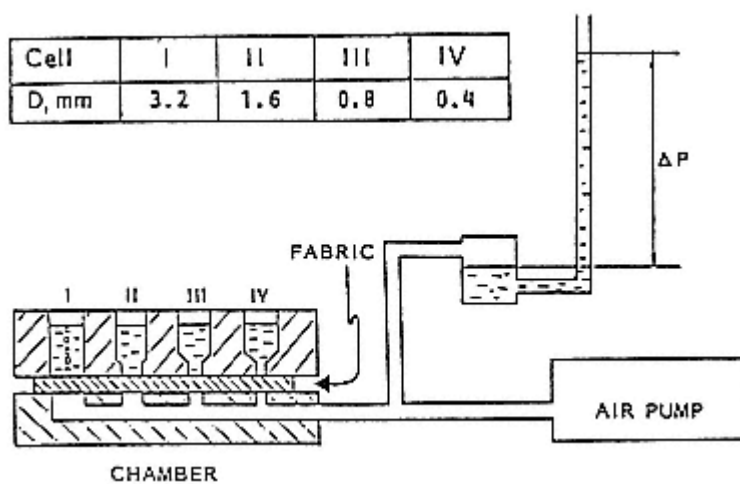


Figure 14
Schematic of apparatus for multiple-scan minimum bubble
pressure measurements.
(From Ref. 12.)

lower section of the apparatus so that they connect to the air inlet below. The same size holes were drilled in the upper plate above the specimen, coincident with their counterparts below.

The entire cell is placed in enough liquid so that the fabric specimen is wetted and liquid is present in each hole above it. Air pressure is increased by pumping until the first bubbles appear in one of the holes. This pressure is recorded to give the effective pore radius through Eq. (3), and that hole is closed with a plug. Additional pressure is then applied until bubbles appear at another hole. The pressure is recorded, the hole is plugged, and the process is continued with the remaining holes. The fabric specimen is then moved so that the holes are located over another portion of the fabric, and the bubble pressures are determined in the same manner. The process is repeated until a sufficiently large area of the material has been scanned. The data are then analyzed statistically to provide a distribution starting with the largest pore (throat) in the sample, and going down to about the mean pore size. Smaller pores cannot be analyzed, but they contribute little to any transport or absorption process.

C—

Applications

The technique can be used to quantify the distribution of the larger pores in a wide range of planar porous materials. In Figure 15 is shown the distribution of large pores in a Millipore membrane filter rated as an 8- μm filter. As can be seen, the material did not reveal the presence of any pores with diameters larger than about 4.8 μm , indicating the margin of safety of this product. It is also noteworthy that the distribution of these large pores is extremely narrow. Similarly narrow pore throat distributions are observed in Figure 16 for a glass fiber mat at three levels of compression.

In Figure 17 are shown the distributions of large pores in a typical woven cotton fabric and in its durable-press treated counterpart. The original purpose of this comparison was to determine whether DP finishing with a cross-linking resin would reduce the pore dimensions. However, the results show that the pores in the DP cotton are actually somewhat larger. This is a direct consequence of the fact that both materials were laundered using conventional home laundry equipment before being analyzed. The untreated cotton fabric shrank more than the DP treated one, and the relative change in fabric dimensions caused the pore dimensions to be greater in the treated material.

VI—

Conclusions

Pore size distributions are the principal factors controlling the extent and rate of absorption of liquids by fibrous networks. Analytical techniques and instrumentation are now available that can determine the effective volumetric capacities and

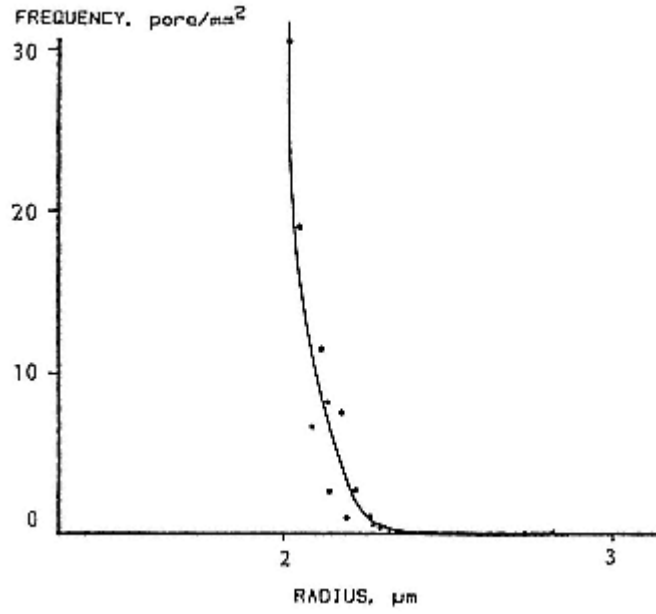


Figure 15
Pore throat size distribution for an 8- μm Millipore membrane.
(From Ref. 12.)

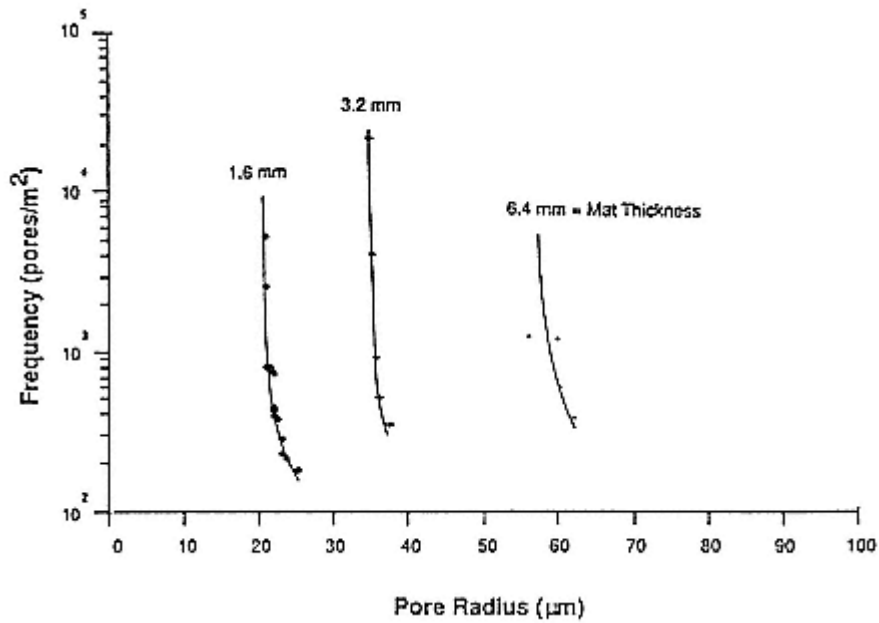


Figure 16
Pore throat distributions for one of the glass-fiber mats described in Fig. 2 at three levels of thickness.
(From Ref. 4.)

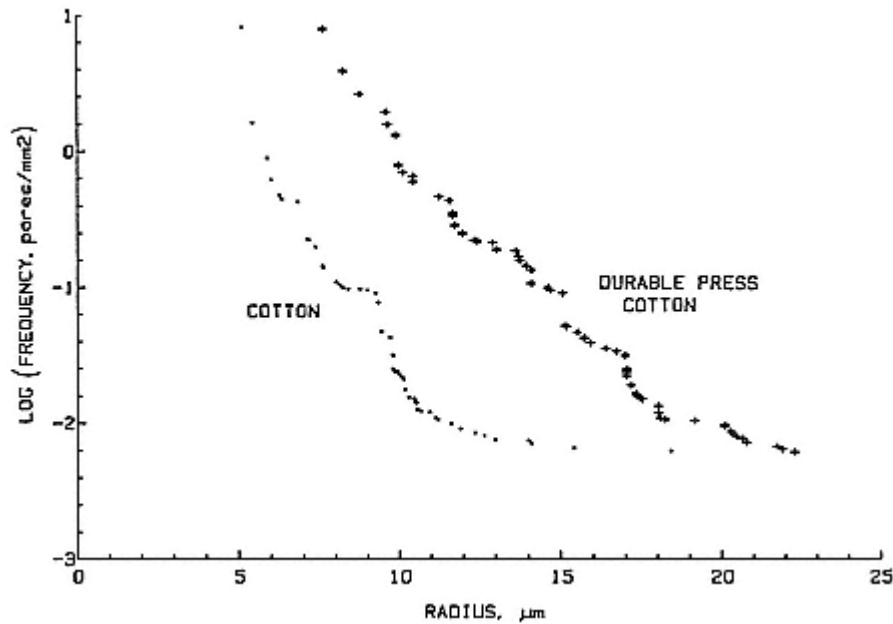


Figure 17
Pore throat distributions for a cotton fabric and for the
same fabric treated with a durable-press resin.
(From Ref. 12.)

throat dimensions of available pores. These techniques are especially useful since they describe the structure of the porous network as it is after exposure to a specific liquid. Porosity values are of little or no use as predictors for absorption performance, since they provide no information about pore structure, and they may overestimate total useful absorption capacities by including inaccessible free volume elements.

References

1. M. Muskat, *The Flow of Homogeneous Fluids Through Porous Media*, J. W. Edwards, Ann Arbor, Mich., 1946.
2. F. A. L. Dullien, *Porous Media—Fluid Transport and Pore Structure*, Academic Press, New York, 1979.
3. A. E. Scheidegger, *The Physics of Flow Through Porous Media*, Macmillan, New York, 1974.
4. D.E. Hirt, K. L. Adams, R. K. Prud'homme, and L. Rebenfeld, In-plane radial fluid flow characterization of fibrous materials, *J. Thermal Insulation* 10:153–172 (1987).
5. M. A. Ioannidis, I. Chatzis, and A. C. Payatakes, A mercury porosimeter for investigating capillary phenomena and microdisplacement mechanisms in capillary networks, *J. Colloid Interface Sci.* 143:22–36 (1991).

6. D. N. Winslow, Advances in experimental techniques for mercury intrusion porosimetry, *Surface and Colloid Science*, Vol. 13 (E. Matijevic and R. J. Good, eds.), Plenum Press, New York, 1984.
7. R. J. Good, The contact angle of mercury on the internal surfaces of porous bodies, *Surface and Colloid Science*, Vol. 13 (E. Matijevic and R. J. Good, eds.), Plenum Press, New York, 1984.
8. B. Miller and I. Tyomkin, An extended range liquid extrusion method for determining pore size distributions, *Textile Res. J.* 56:35–40 (1986).
9. A. A. Burgeni and C. Kapur, Capillary sorption equilibria in fiber masses, *Textile Res. J.* 37:356–366 (1967).
10. B. Miller and I. Tyomkin, Liquid porosimetry: New methodology and applications, *J. Colloid Interface Sci.* 162:163–170 (1994).
11. D. M. Klein, I. Tyomkin, B. Miller, and L. Rebenfeld, Pore volume distribution of artificial skin by liquid extrusion analysis, *J. Appl. Biomater.* 1:137–141 (1990).
12. B. Miller, I. Tyomkin, and J. A. Wehner, Quantifying the porous structure of fabrics for filtration applications, *Fluid Filtration: Gas*, Vol. I, ASTM STP 975 (R. R. Raber, ed.), American Society for Testing and Materials, Philadelphia, 1986.